Classification, photo-z and environment of X-ray selected sources in the XMM-LSS field

O.Melnyk, M.Plionis, A.Elyiv, M.Salvato,
L. Chiappetti, N. Clerc, P. Gandhi, M.Pierre,
T. Sadibekova, A. Pospieszalska-Surdej and J. Surdej

Content

Content

- Classification of the sources

Content

- Classification of the sources
- Photo-z estimation

Content

- Classification of the sources
- Photo-z estimation
- Local overdensity measurements

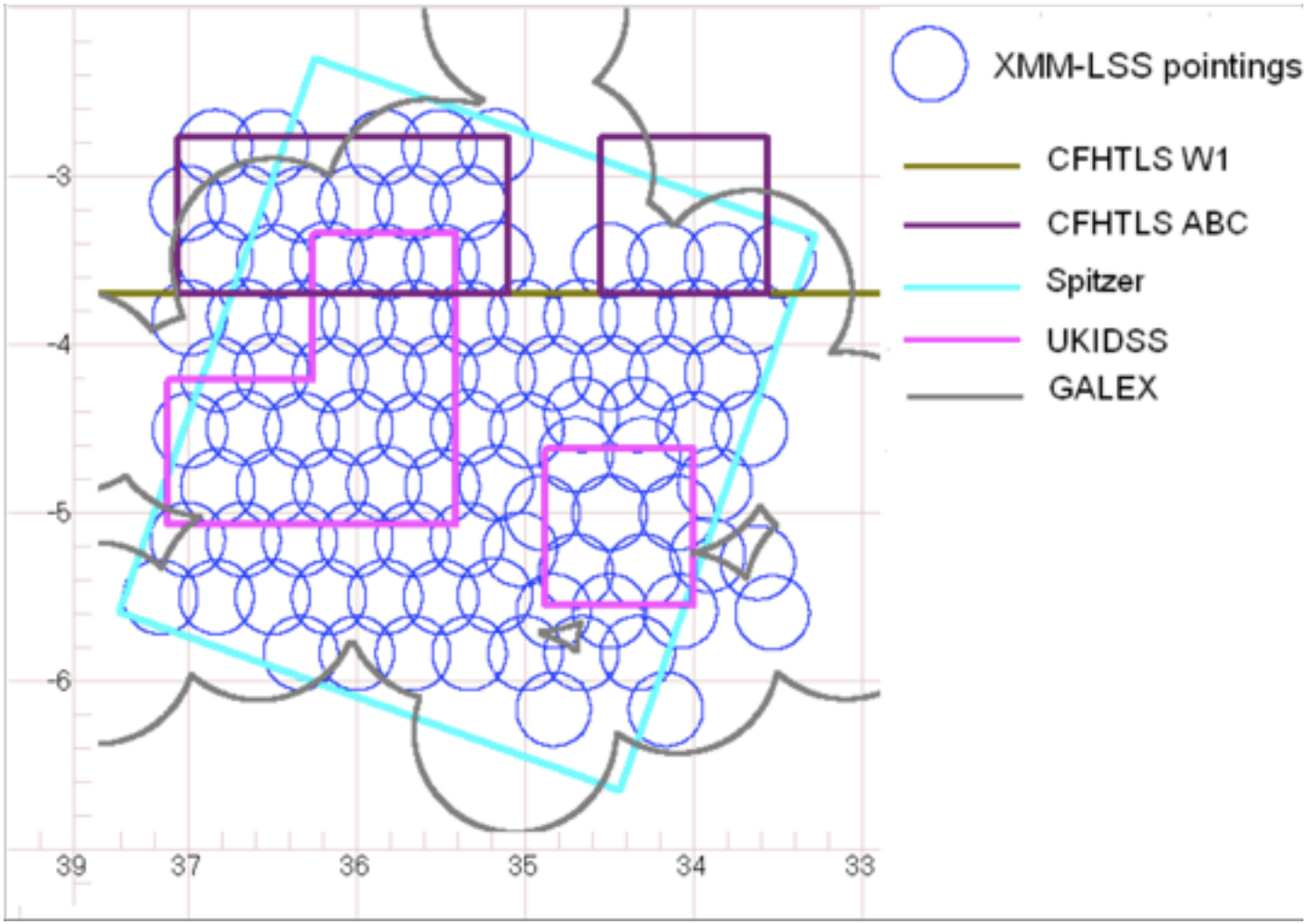
XMM-LSS pointings
CFHTLS W1
CFHTLS ABC
Spitzer
UKIDSS
GALEX
-3
-4
-5
-6
39
37
36
35
34
33

Morphological classification

N=5142
With optical counterparts
Good fields
Best ranked counterparts

- Extended object (ext)
- Point-like object (ptl)
- STARs
- Very faint/Invisible/ Misclassified (mcl)

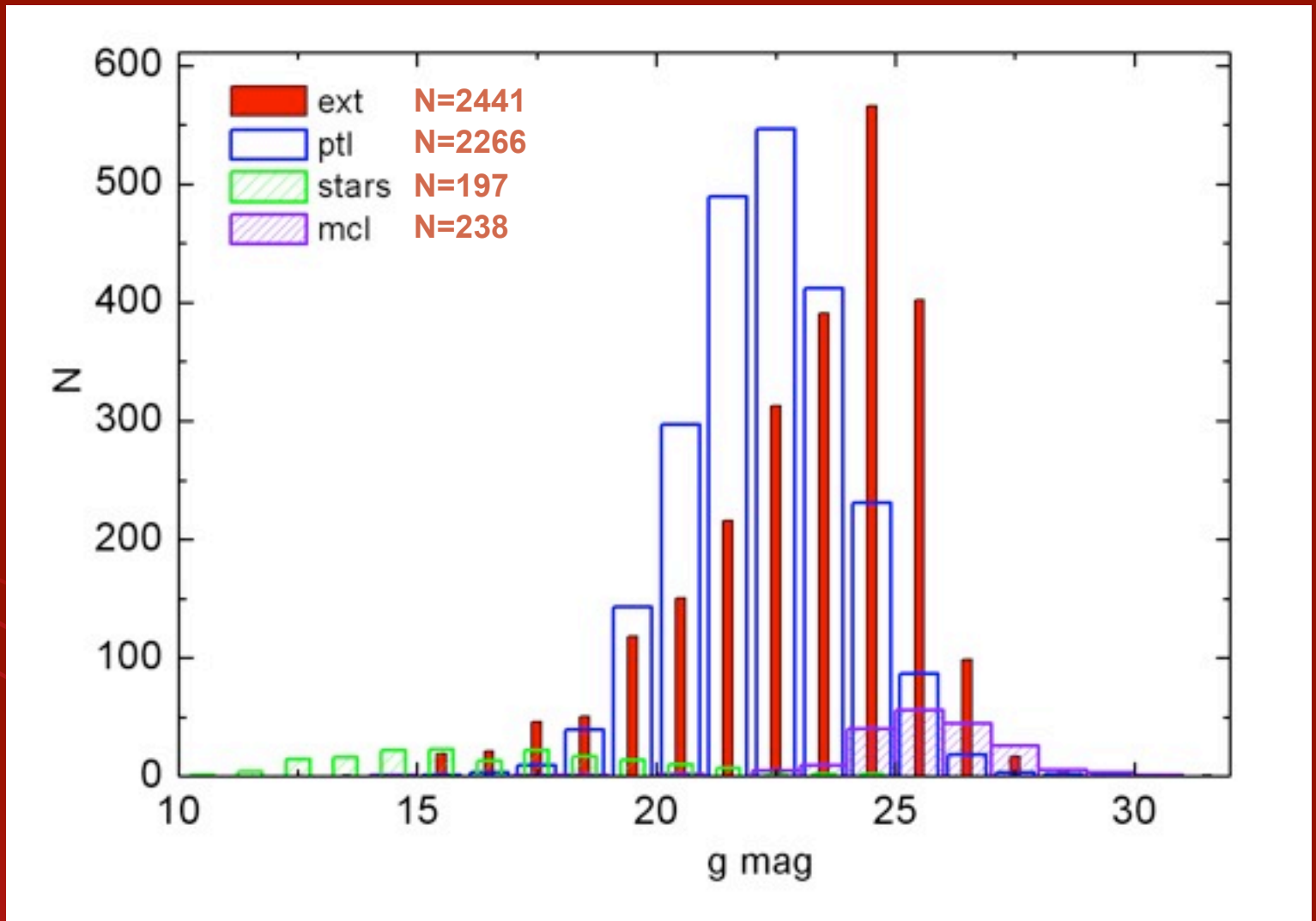
ext N=2441
ptl N=2266
stars N=197
mcl N=238
N
g mag
0
100
200
300
400
500
600
10
15
20
25
30

Flow-chart by Salvato et al. 2011

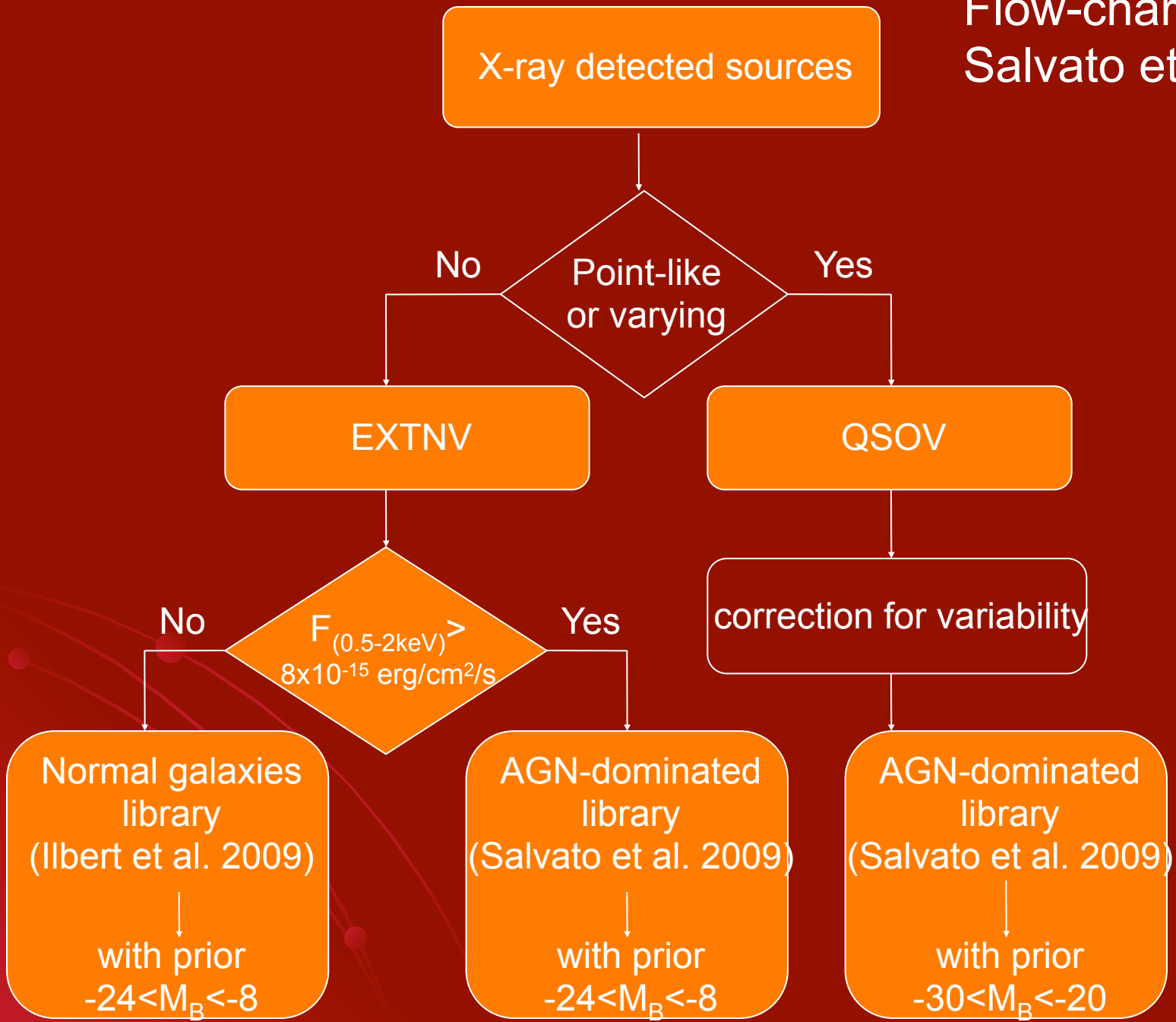

AB photometric system, total mags, Galactic extinction correction; max 11 bands: u,g,r,i,z, J,K, 3.6 & 4.5 μm NUV and FUV

Modifications to Flow-chart by Salvato et al. 2011

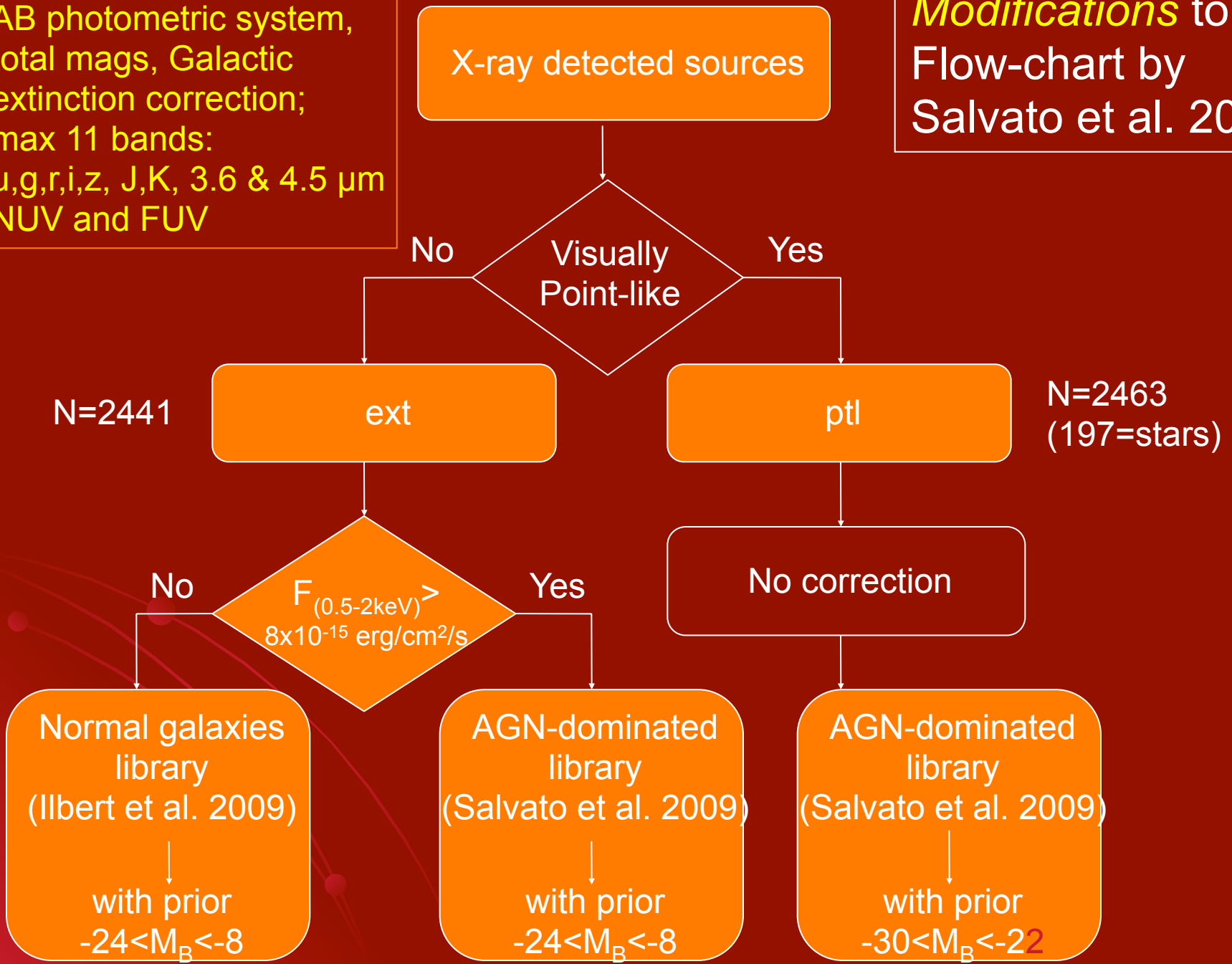

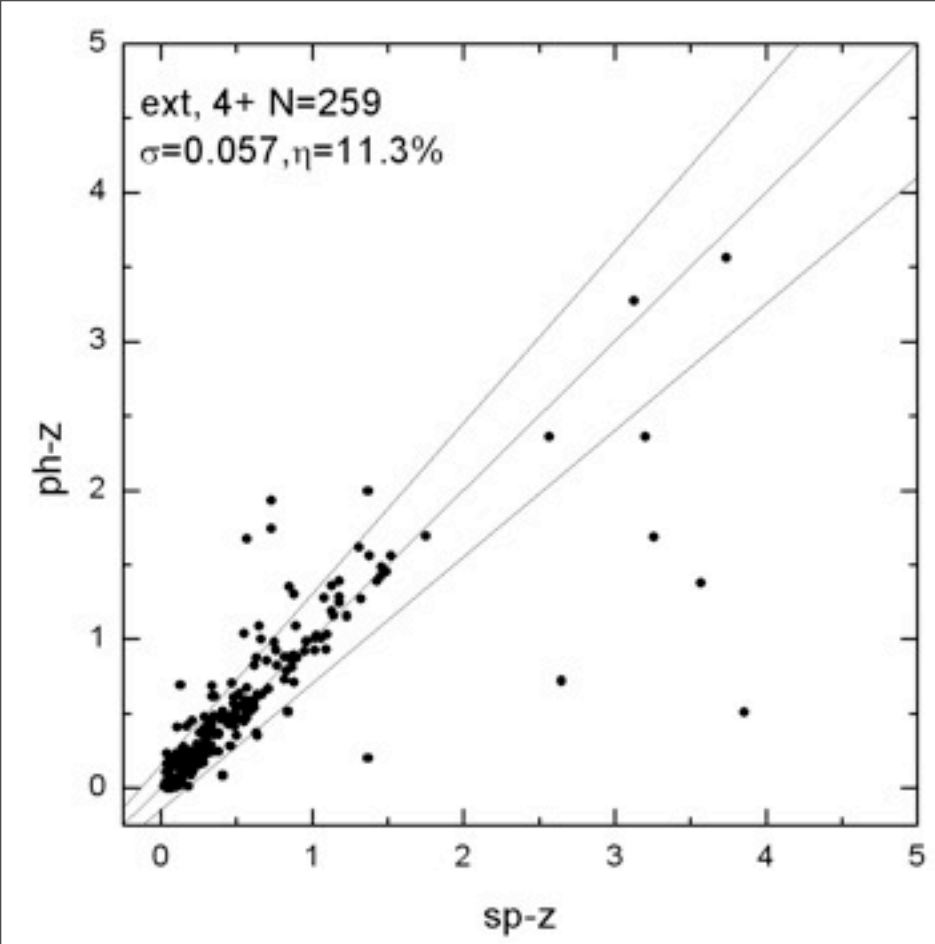
ext, 4+ N=259
σ=0.057,η=11.3%
ph-z
sp-z
0
1
2
3
4
5

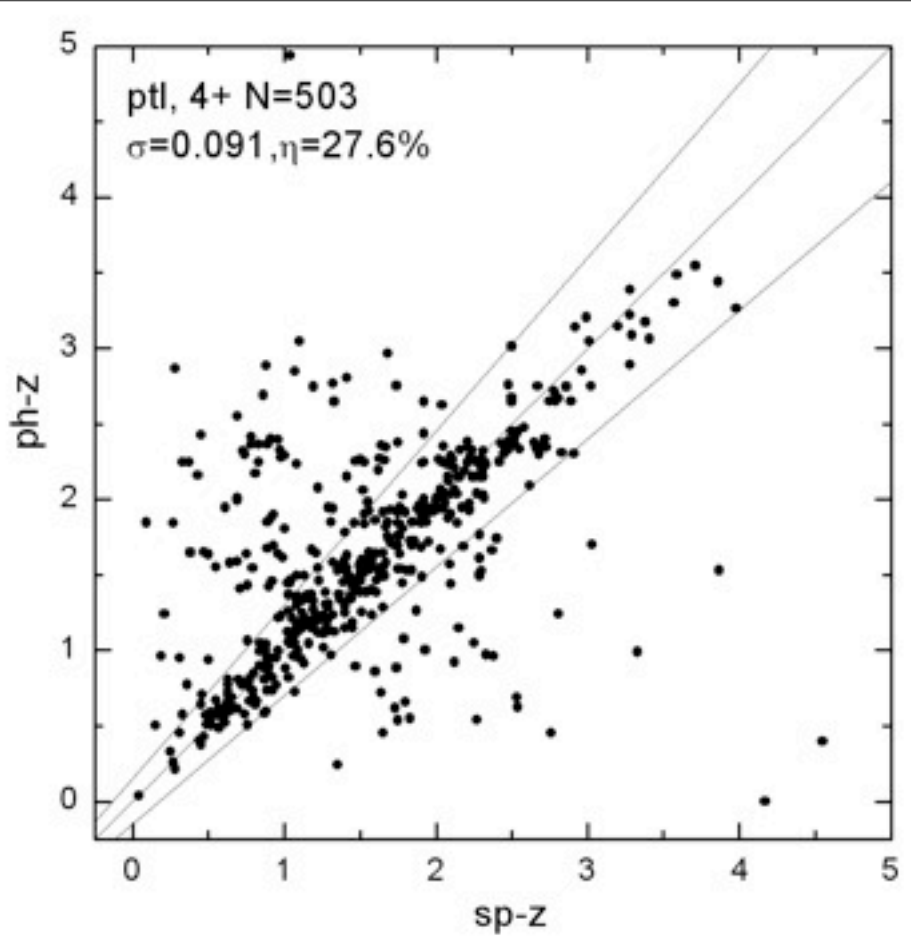
ptl, 4+ N=503
σ=0.091,η=27.6%
ph-z
sp-z
0
1
2
3
4
5

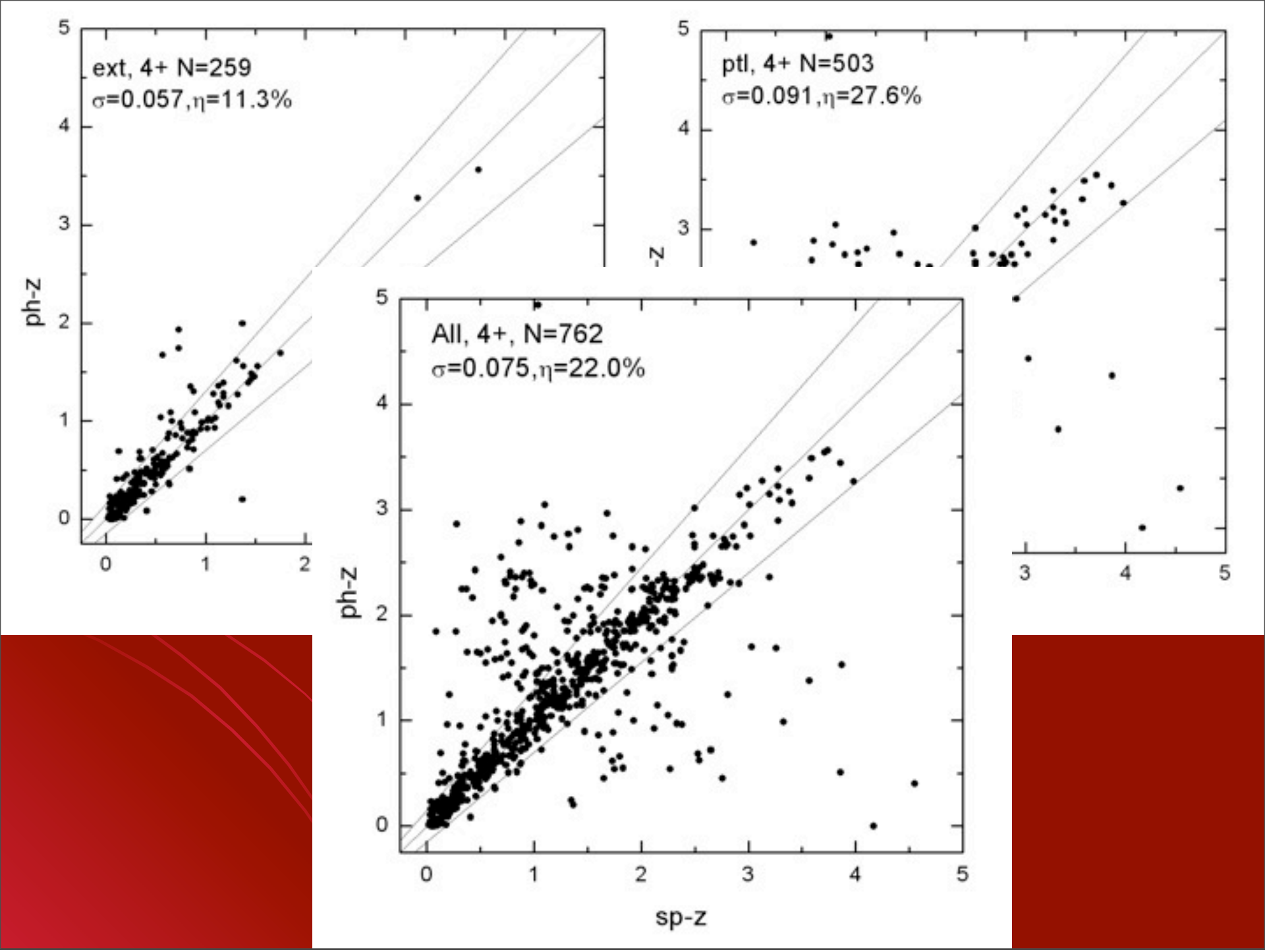
ext, 4+ N=259
σ=0.057,η=11.3%
ptl, 4+ N=503
σ=0.091,η=27.6%
All, 4+, N=762
σ=0.075,η=22.0%
ph-z
sp-z

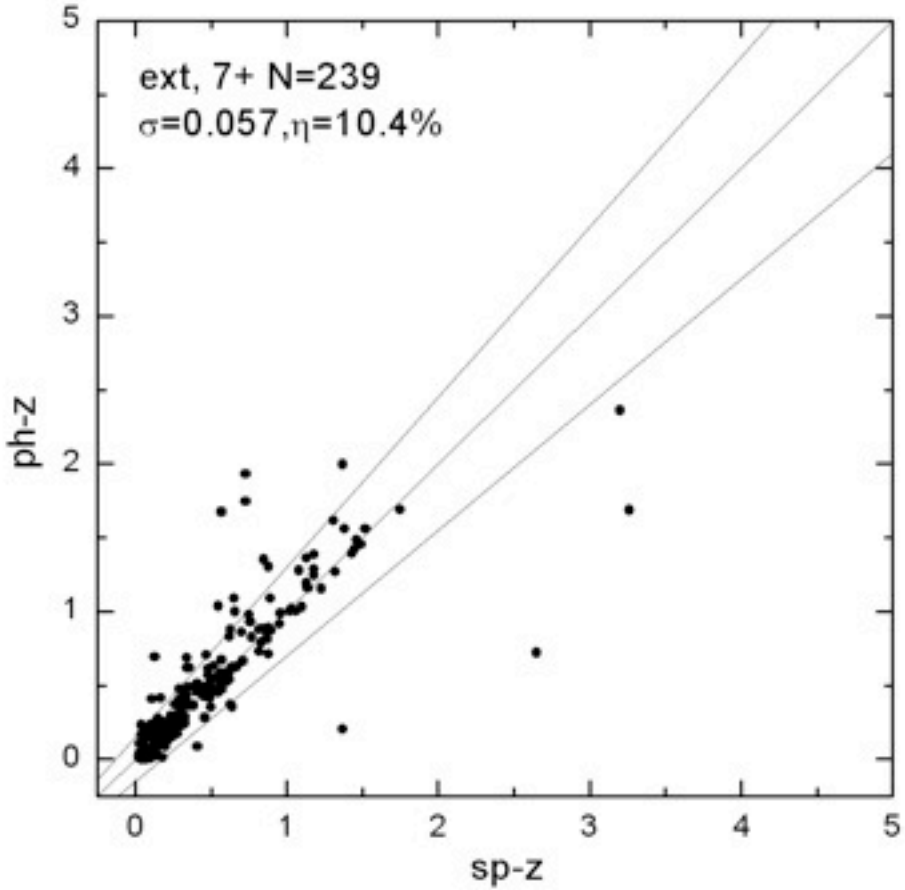
ext, 7+ N=239
σ=0.057,η=10.4%
ph-z
sp-z
0
1
2
3
4
5

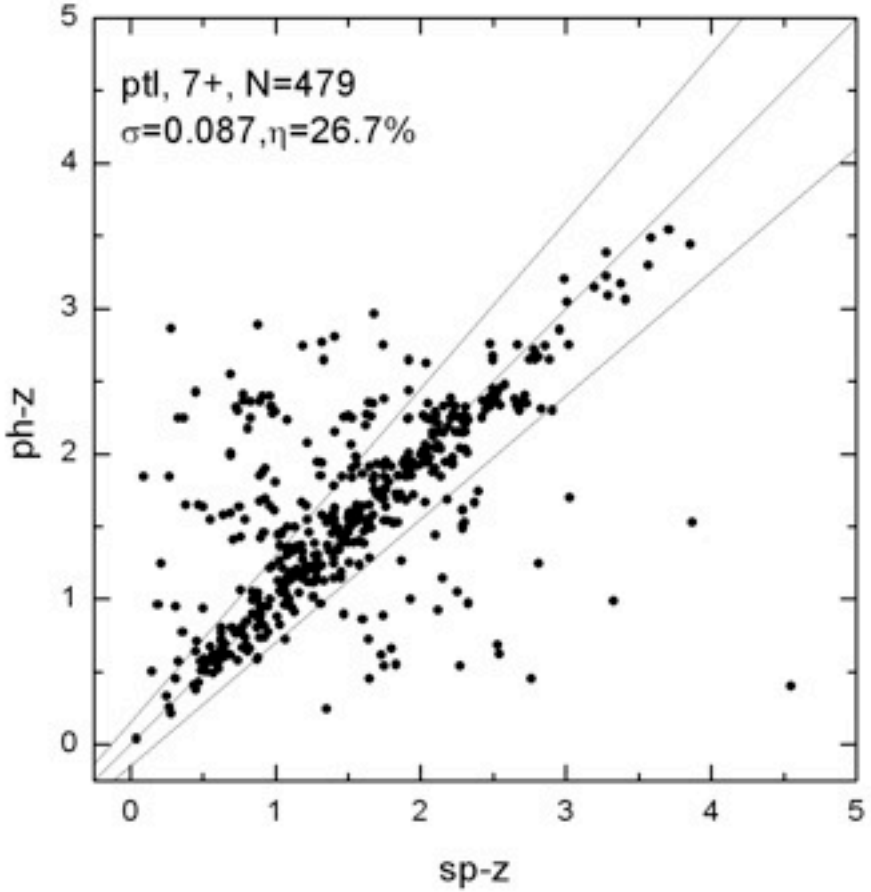
ptl, 7+, N=479
σ=0.087,η=26.7%
ph-z
sp-z
0
1
2
3
4
5

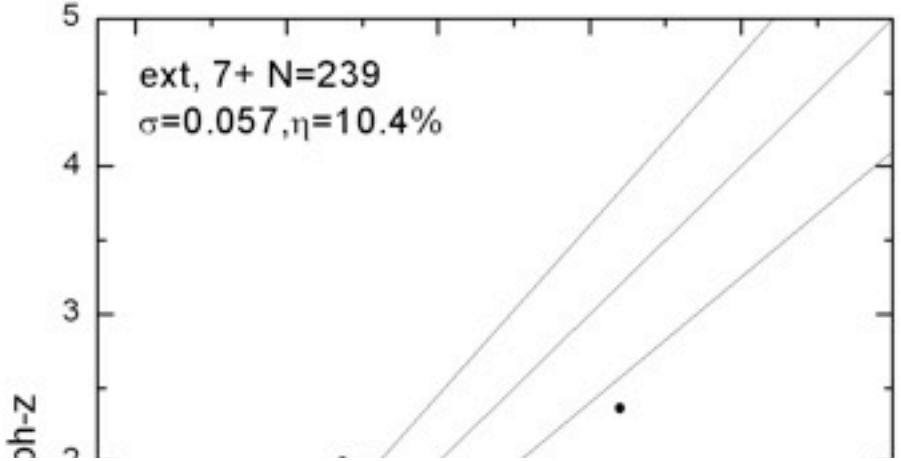
ext, 7+ N=239
σ=0.057,η=10.4%
ph-z

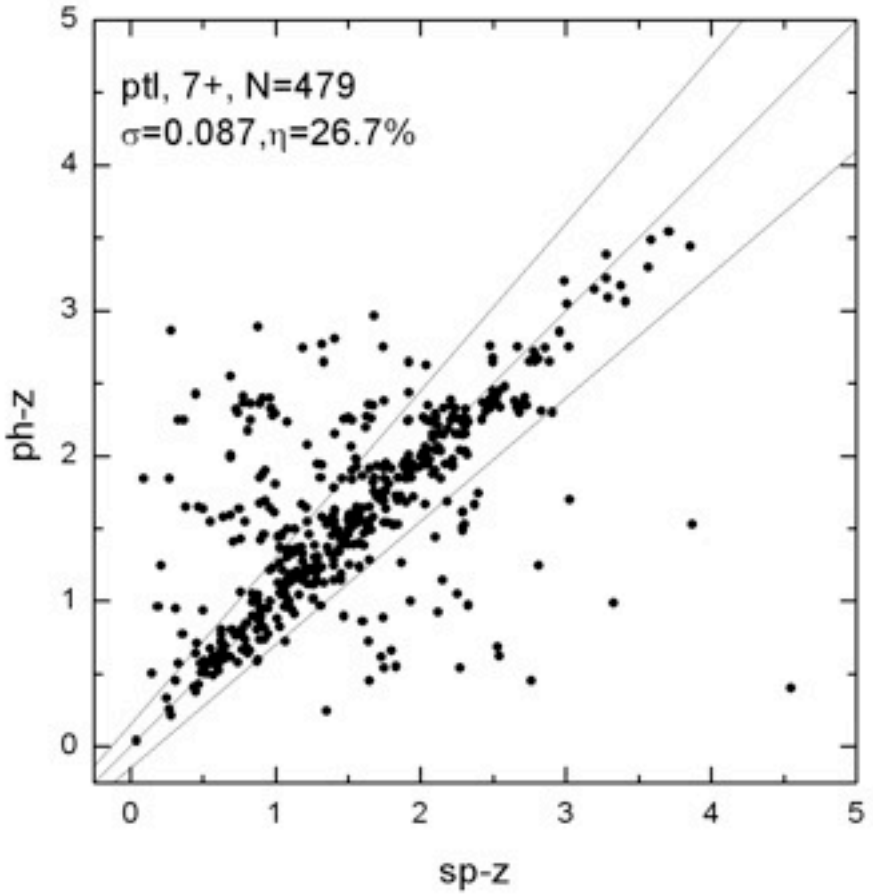
ptl, 7+, N=479
σ=0.087,η=26.7%
ph-z
sp-z

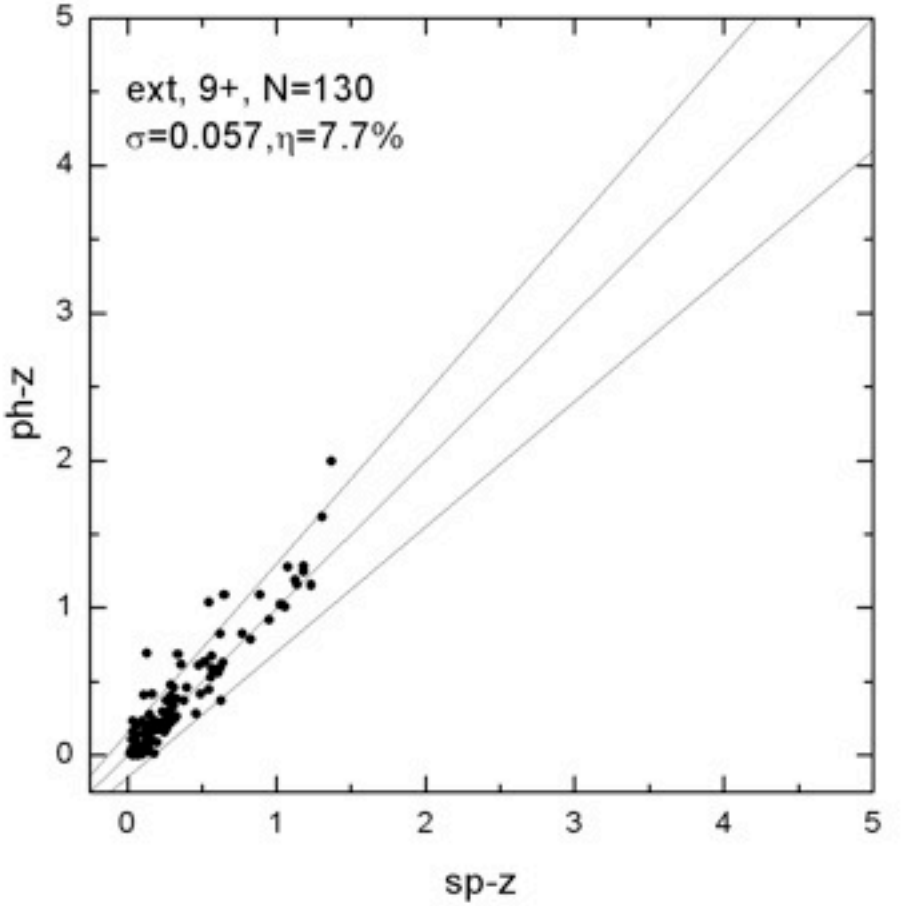
ext, 9+, N=130
σ=0.057,η=7.7%
ph-z
sp-z

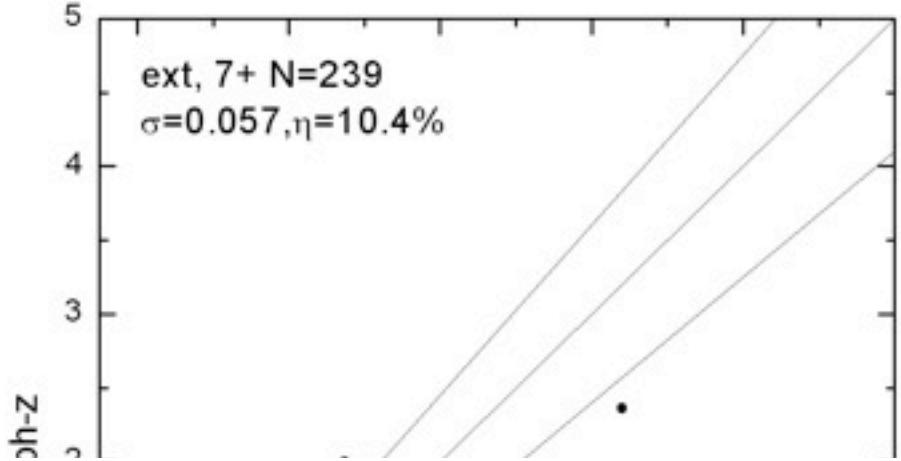
ext, 7+ N=239
σ=0.057,η=10.4%

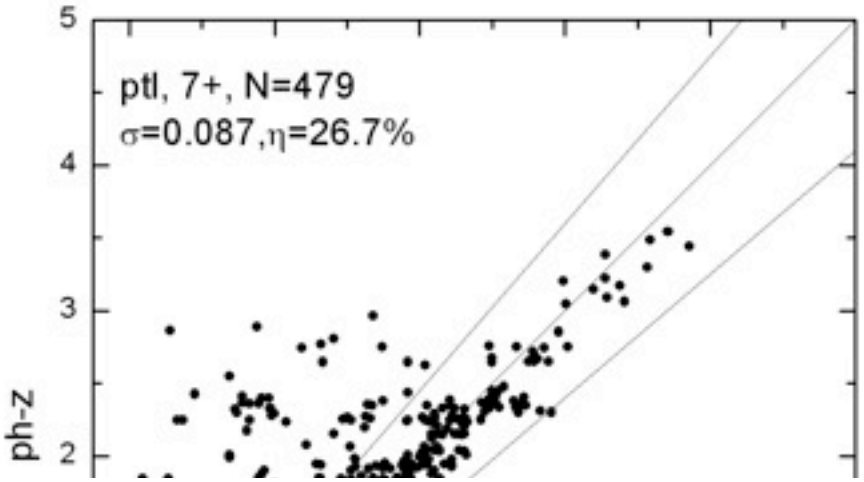
ptl, 7+, N=479
σ=0.087,η=26.7%
ph-z

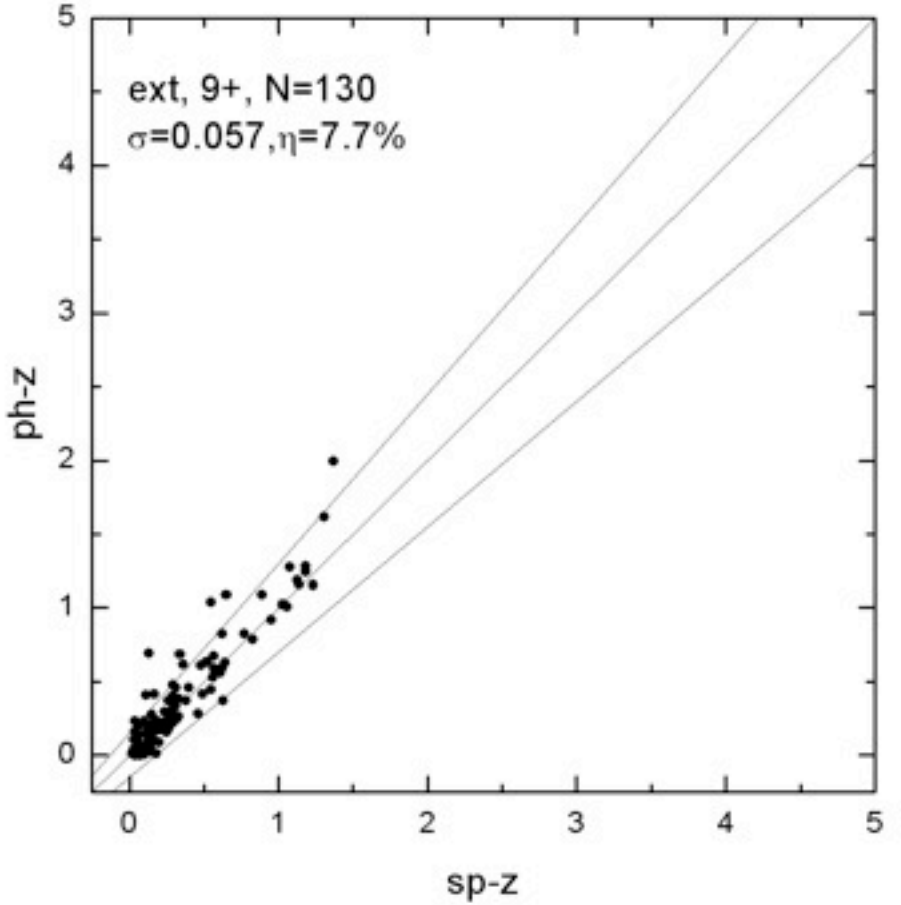
ext, 9+, N=130
σ=0.057,η=7.7%
ph-z
sp-z

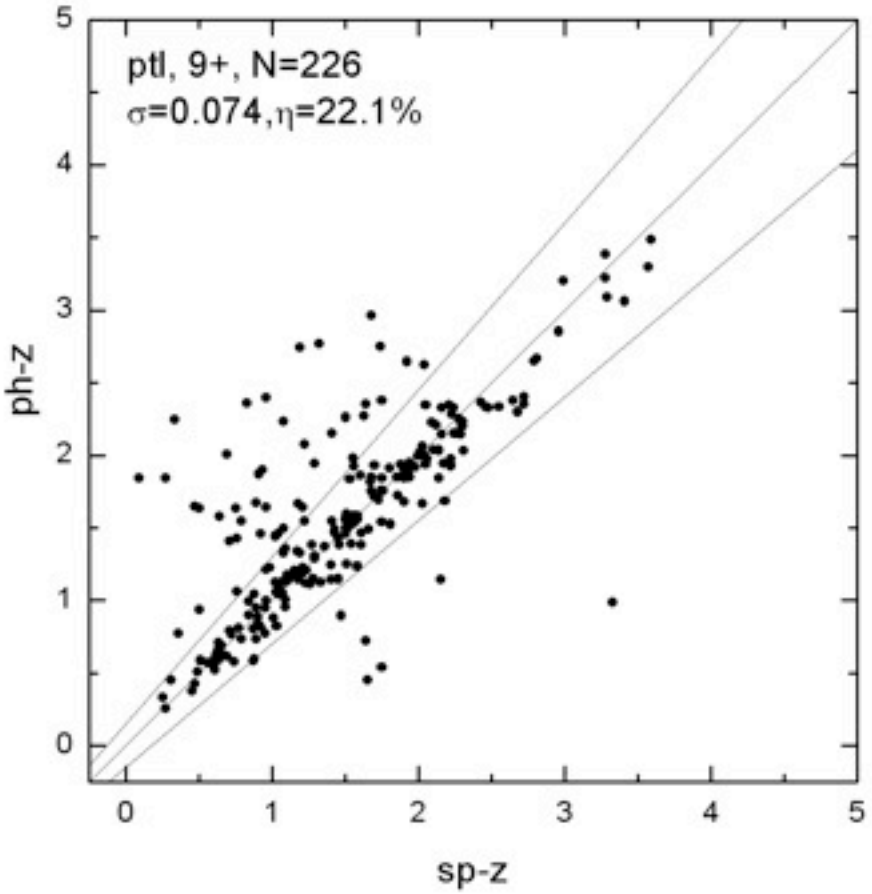
ptl, 9+, N=226
σ=0.074,η=22.1%
ph-z
sp-z

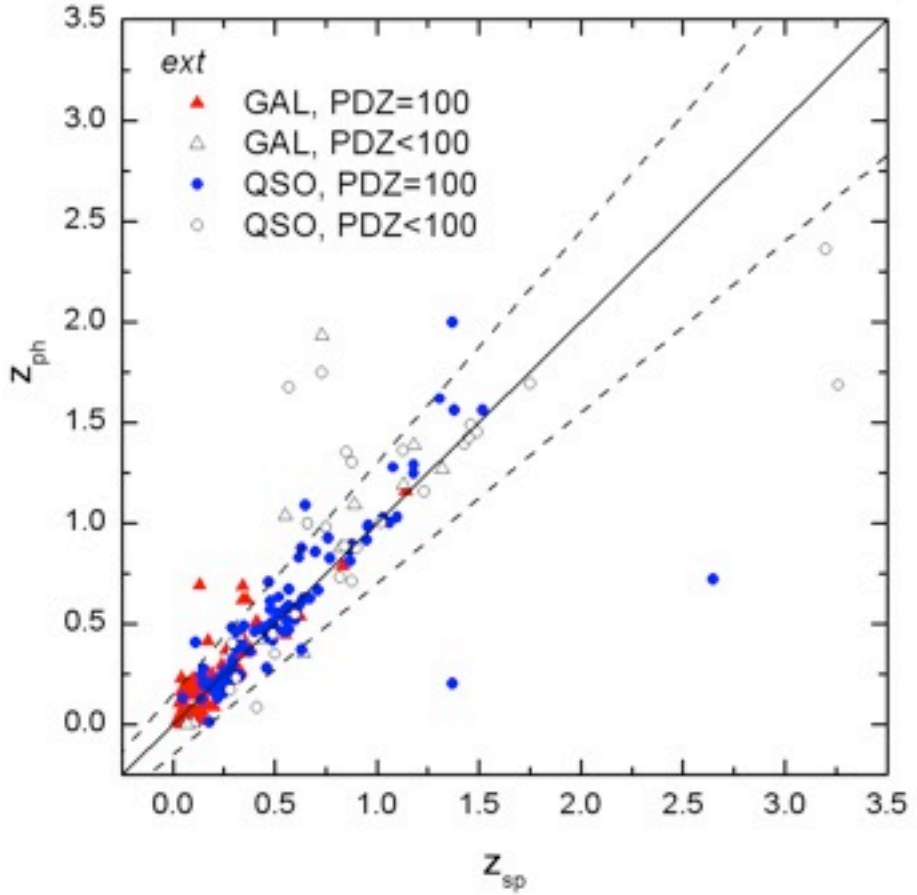

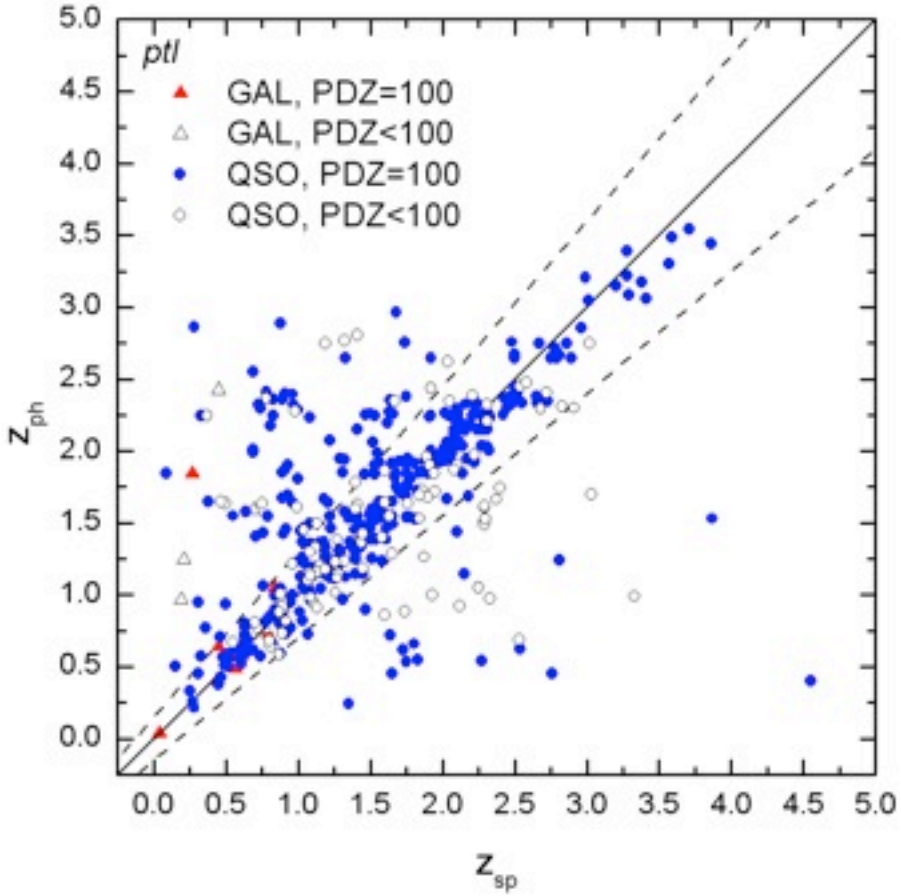

ext, N=193
PDZ=100
σ=0.052 , η=7.3%

ptl, N=373
PDZ=100
σ=0.074 , η=23.9%

Sample	N_{tot} (N_{sp})	*ext* $\sigma_{\Delta z/(1+z_{sp})}$	η,%
4+ bands	2250 (259)	0.057	11.2
7+ bands	1339 (239)	0.057	10.4
9+ bands	415 (130)	0.057	7.7
$7+_{PDZ=100}$	749 (193)	0.052	7.3
$7+_{PDZ=100,i<22}$	819 (209)	0.057	8.1
$7+_{PDZ=100,z_{ph}<0.7}$	478 (162)	0.052	5.6

Sample	N_{tot} (N_{sp})	*ptl* $\sigma_{\Delta z/(1+z_{sp})}$	η,%
4+ bands	2201 (503)	0.091	27.6
7+ bands	1725 (479)	0.087	26.7
9+ bands	570 (226)	0.074	22.1
$7+_{PDZ=100}$	1072 (373)	0.074	23.9
$7+_{PDZ=100,i<22}$	1278 (334)	0.076	25.0
$7+_{PDZ=100,z_{ph}<0.7}$	155 (46)	0.076	28.2

Sample	N_{tot} (N_{sp})	*all* $\sigma_{\Delta z/(1+z_{sp})}$	η,%
4+ bands	4451 (762)	0.075	22.0
7+ bands	3064 (718)	0.073	21.3
9+ bands	985 (356)	0.063	16.9
$7+_{PDZ=100}$	1821 (556)	0.063	18.2
$7+_{PDZ=100,i<22}$	2097 (635)	0.071	20.0
$7+_{PDZ=100,z_{ph}<0.7}$	633 (208)	0.056	10.6

		ext	
Sample	N_{tot} (N_{sp})	$\sigma_{\Delta z/(1+z_{sp})}$	η,%
4+ bands	2250 (259)	0.057	11.2
7+ bands	1339 (239)	0.057	10.4
9+ bands	415 (130)	0.057	7.7
$7+_{PDZ=100}$	749 (193)	0.052	7.3
$7+_{PDZ=100,i<22}$	819 (209)	0.057	8.1
$7+_{PDZ=100,z_{ph}<0.7}$	478 (162)	0.052	5.6
		ptl	
Sample	N_{tot} (N_{sp})	$\sigma_{\Delta z/(1+z_{sp})}$	η,%
4+ bands	2201 (503)	0.091	27.6
7+ bands	1725 (479)	0.087	26.7
9+ bands	570 (226)	0.074	22.1
$7+_{PDZ=100}$	1072 (373)	0.074	23.9
$7+_{PDZ=100,i<22}$	1278 (334)	0.076	25.0
$7+_{PDZ=100,z_{ph}<0.7}$	155 (46)	0.076	28.2
		all	
Sample	N_{tot} (N_{sp})	$\sigma_{\Delta z/(1+z_{sp})}$	η,%
4+ bands	4451 (762)	0.075	22.0
7+ bands	3064 (718)	0.073	21.3
9+ bands	985 (356)	0.063	16.9
$7+_{PDZ=100}$	1821 (556)	0.063	18.2
$7+_{PDZ=100,i<22}$	2097 (635)	0.071	20.0
$7+_{PDZ=100,z_{ph}<0.7}$	633 (208)	0.056	10.6

Sample	N_{tot} (N_{sp})	*ext* $\sigma_{\Delta z/(1+z_{sp})}$	η,%
4+ bands	2250 (259)	0.057	11.2
7+ bands	1339 (239)	0.057	10.4
9+ bands	415 (130)	0.057	7.7
$7+_{PDZ=100}$	749 (193)	0.052	7.3
$7+_{PDZ=100,i<22}$	819 (209)	0.057	8.1
$7+_{PDZ=100,z_{ph}<0.7}$	478 (162)	0.052	5.6
Sample	N_{tot} (N_{sp})	*ptl* $\sigma_{\Delta z/(1+z_{sp})}$	η,%
4+ bands	2201 (503)	0.091	27.6
7+ bands	1725 (479)	0.087	26.7
9+ bands	570 (226)	0.074	22.1
$7+_{PDZ=100}$	1072 (373)	0.074	23.9
$7+_{PDZ=100,i<22}$	1278 (334)	0.076	25.0
$7+_{PDZ=100,z_{ph}<0.7}$	155 (46)	0.076	28.2
Sample	N_{tot} (N_{sp})	*all* $\sigma_{\Delta z/(1+z_{sp})}$	η,%
4+ bands	4451 (762)	0.075	22.0
7+ bands	3064 (718)	0.073	21.3
9+ bands	985 (356)	0.063	16.9
$7+_{PDZ=100}$	1821 (556)	0.063	18.2
$7+_{PDZ=100,i<22}$	2097 (635)	0.071	20.0
$7+_{PDZ=100,z_{ph}<0.7}$	633 (208)	0.056	10.6

Sample	N_{tot} (N_{sp})	*ext* $\sigma_{\Delta z/(1+z_{sp})}$	η,%
4+ bands	2250 (259)	0.057	11.2
7+ bands	1339 (239)	0.057	10.4
9+ bands	415 (130)	0.057	7.7
$7+_{PDZ=100}$	749 (193)	0.052	7.3
$7+_{PDZ=100,i<22}$	819 (209)	0.057	8.1
$7+_{PDZ=100,z_{ph}<0.7}$	478 (162)	0.052	5.6

Sample	N_{tot} (N_{sp})	*ptl* $\sigma_{\Delta z/(1+z_{sp})}$	η,%
4+ bands	2201 (503)	0.091	27.6
7+ bands	1725 (479)	0.087	26.7
9+ bands	570 (226)	0.074	22.1
$7+_{PDZ=100}$	1072 (373)	0.074	23.9
$7+_{PDZ=100,i<22}$	1278 (334)	0.076	25.0
$7+_{PDZ=100,z_{ph}<0.7}$	155 (46)	0.076	28.2

Sample	N_{tot} (N_{sp})	*all* $\sigma_{\Delta z/(1+z_{sp})}$	η,%
4+ bands	4451 (762)	0.075	22.0
7+ bands	3064 (718)	0.073	21.3
9+ bands	985 (356)	0.063	16.9
$7+_{PDZ=100}$	1821 (556)	0.063	18.2
$7+_{PDZ=100,i<22}$	2097 (635)	0.071	20.0
$7+_{PDZ=100,z_{ph}<0.7}$	633 (208)	0.056	10.6

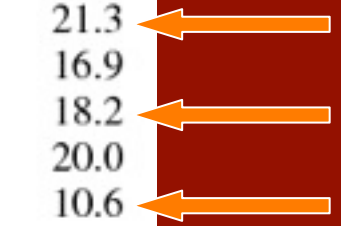

The COSMOS test

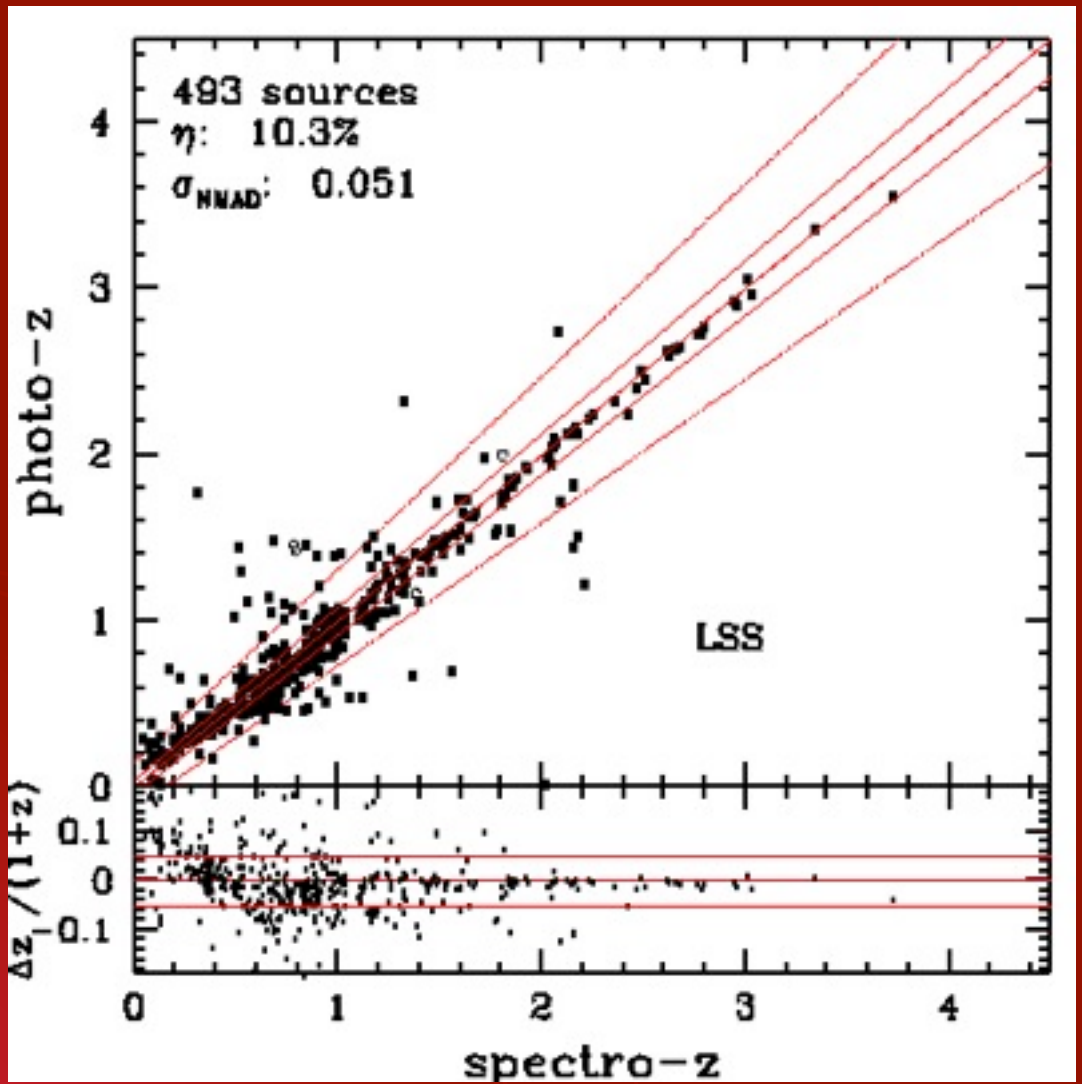

Band	LSS	COSMOS
u	25.3	~26.5
g	25.5	~26.5
r	24.8	~26.5
i	24.5	~26.5
z	23.6	~26.5
J	22.9	23.5
K	23.1	23.5
3.6	21.7	23.9
4.5	21.4	22
NUV	25	25
FUV	25	25

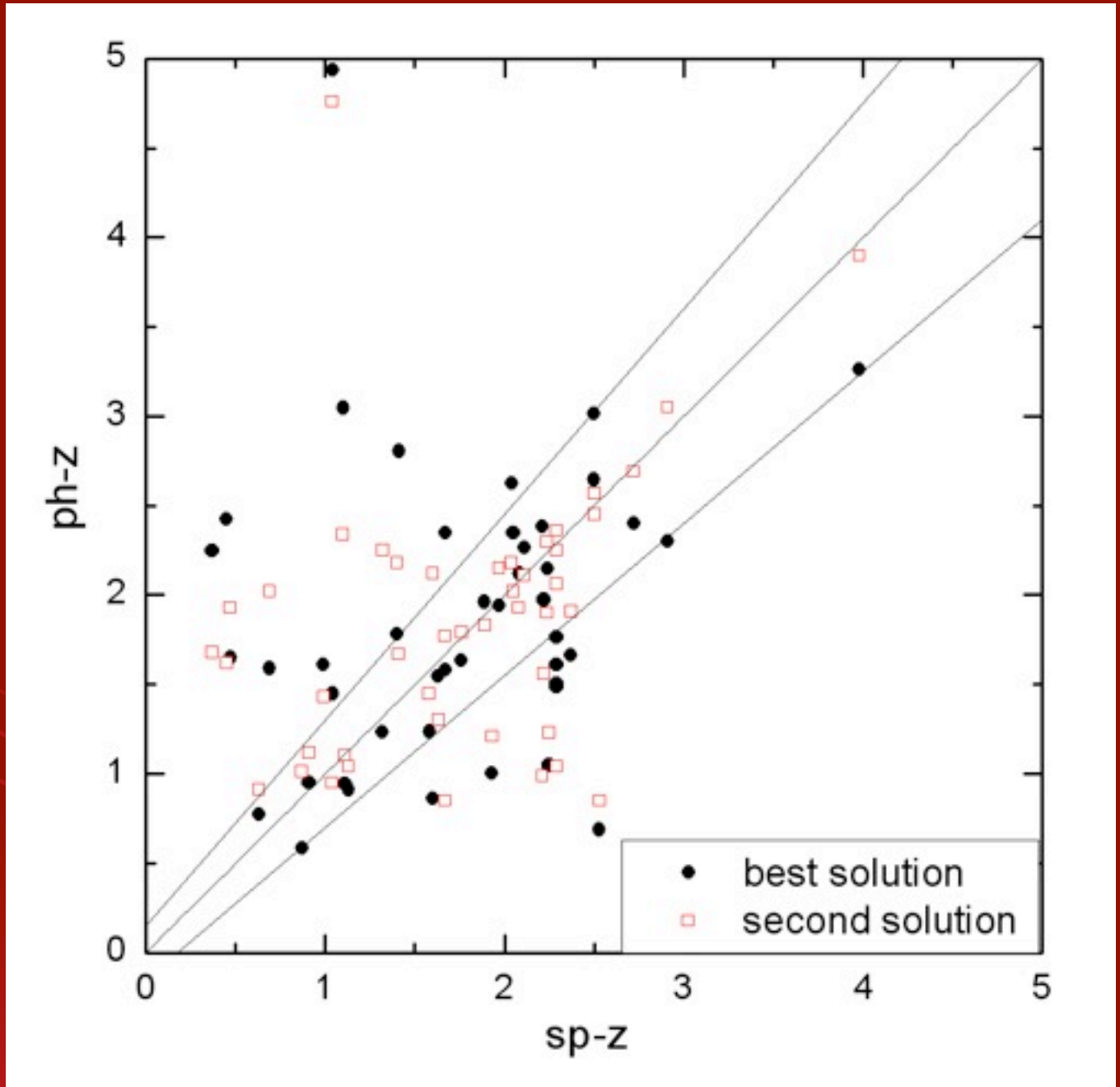
ph-z
sp-z
0
1
2
3
4
5
best solution
second solution

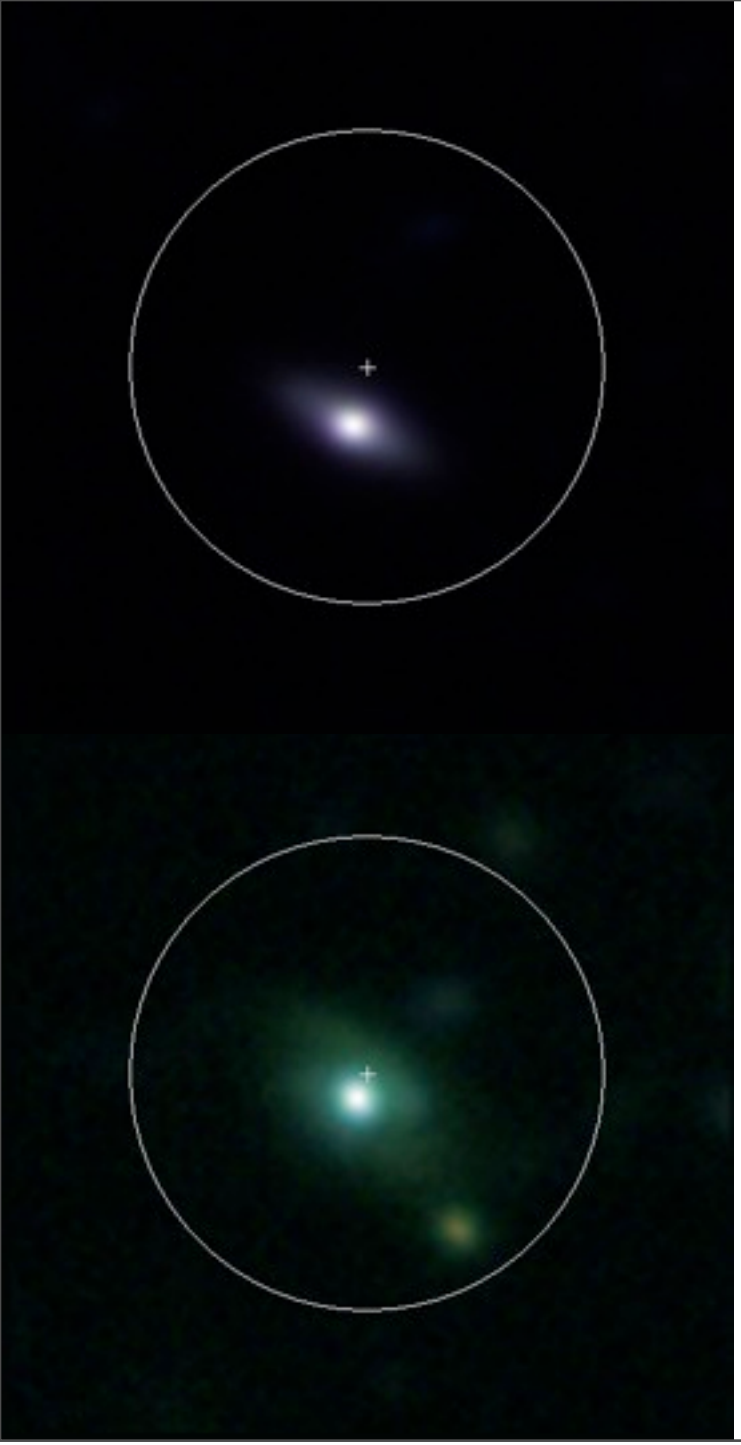

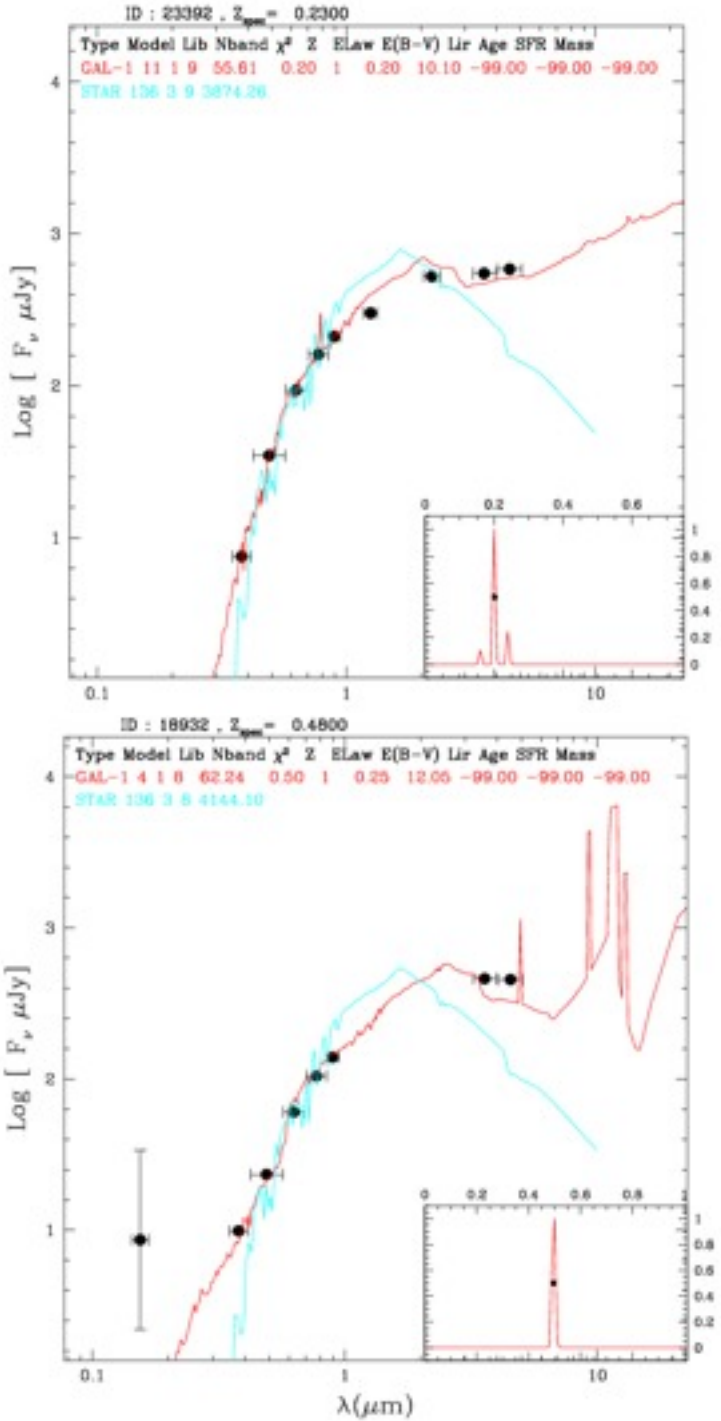

92.2% of ext with normal Galaxy templates

78.8% of ptl with AGN/QSO templates

X-ray luminosity vs. z

N=3081 (1983)

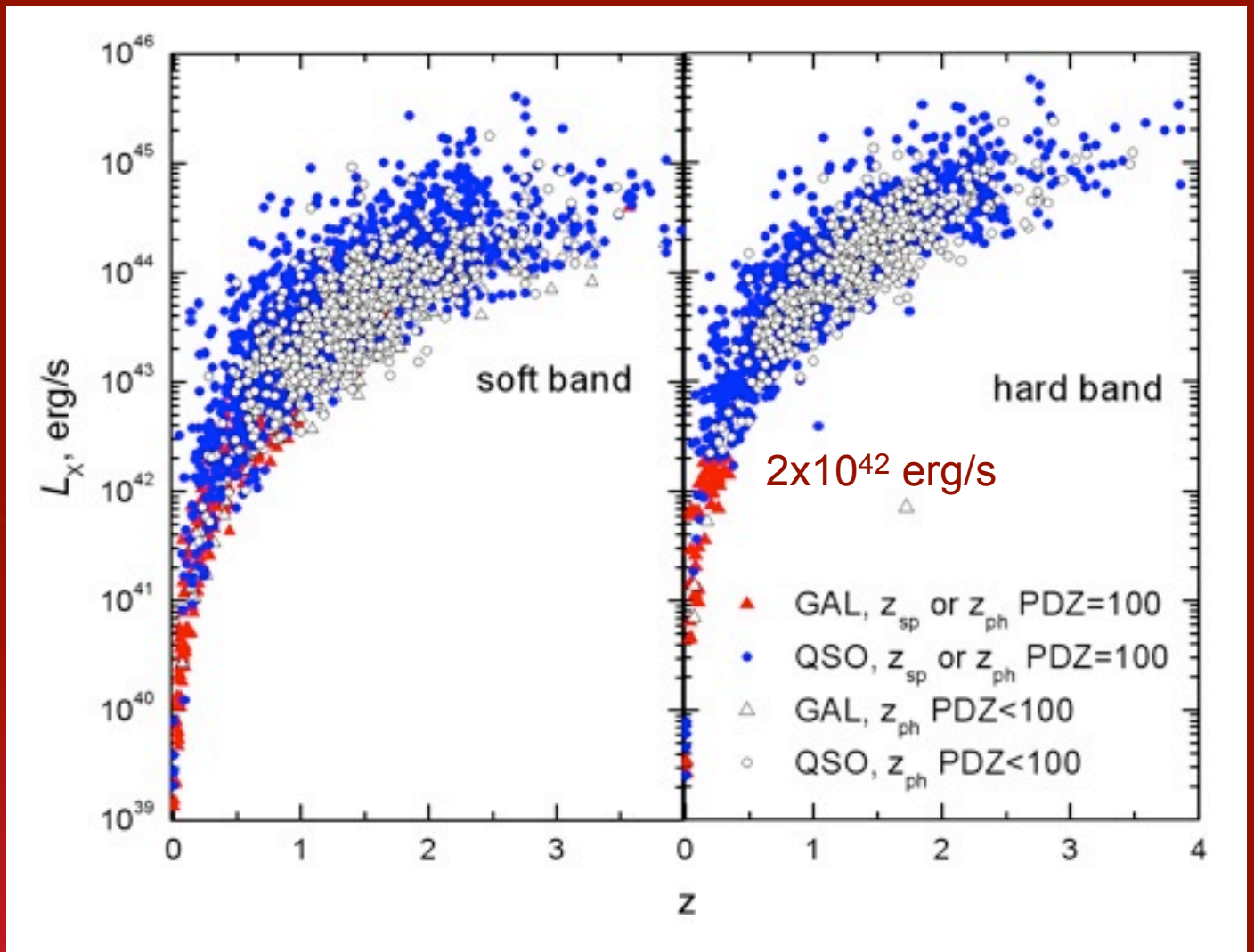

Sp-z or ph-z with 7+ bands

668 (82%) ext

159 (18%) ptl

817 GALs

676 (30%) ext

1578 (70%) ptl

2254 QSOs

Redshift distribution

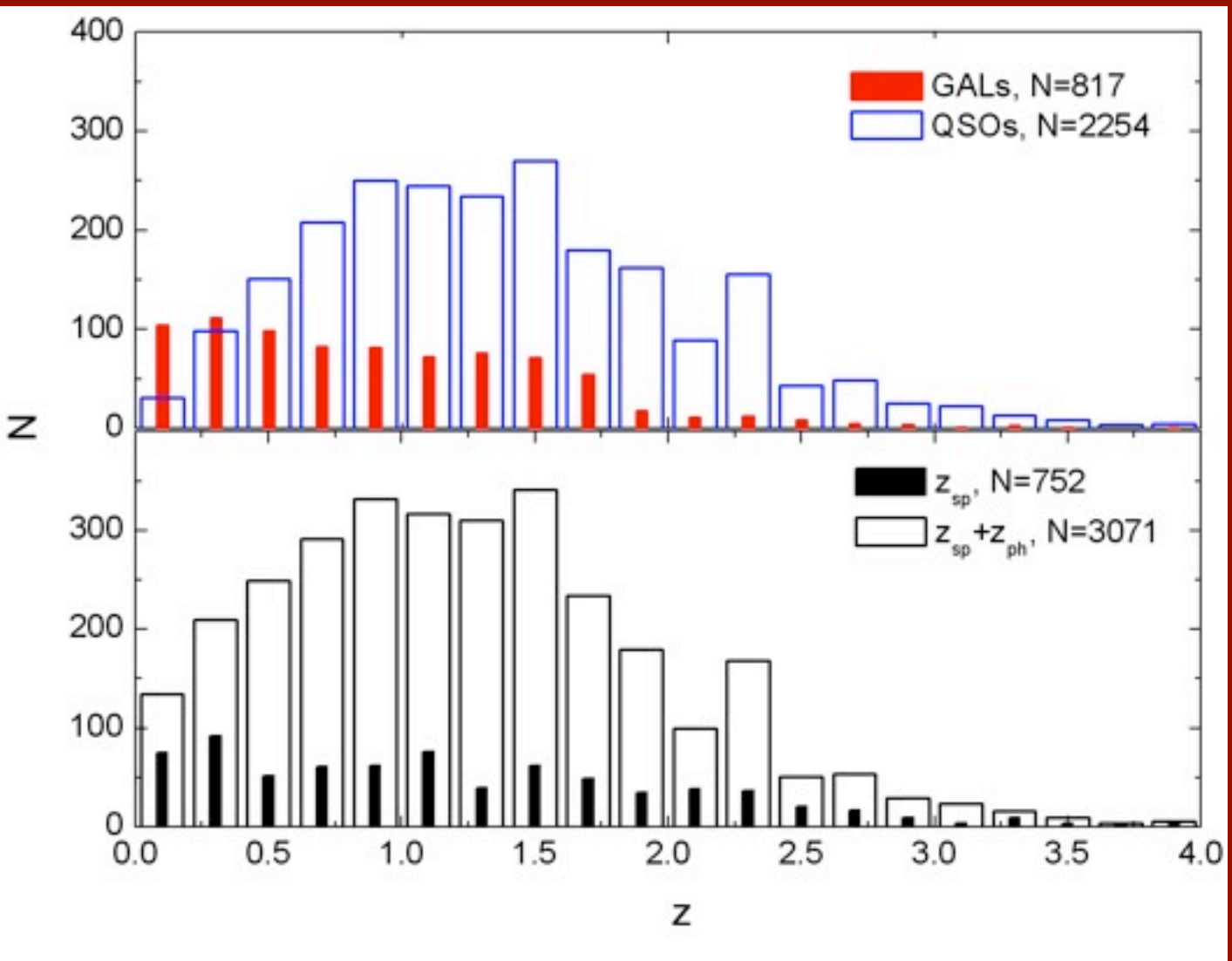

$Z_{med}(GAL)=0.81$

$Z_{med}(QSO)=1.31$

$Z_{med}(ALL)=1.2$

X-ray luminosity vs. magnitude

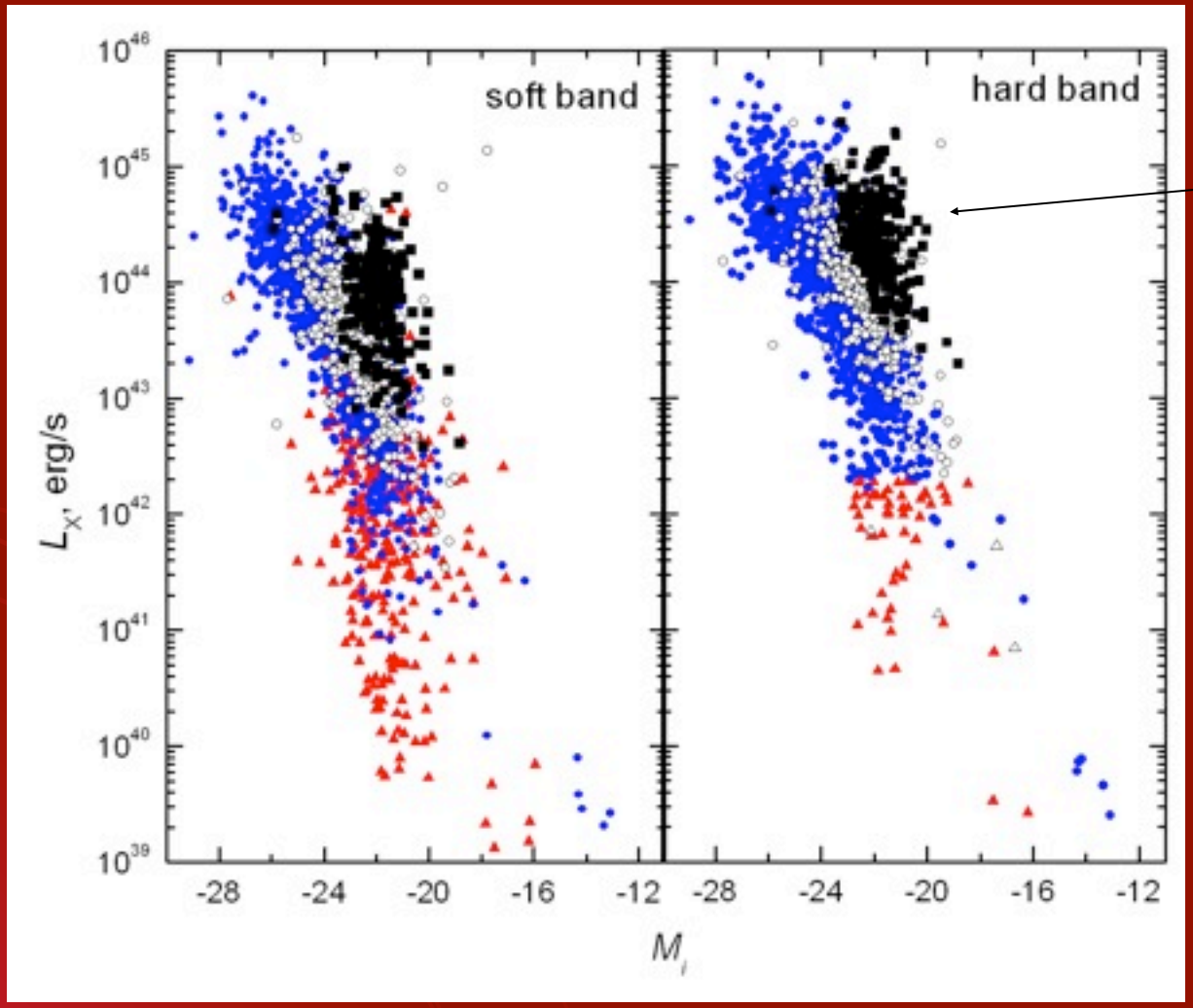

X/O>10

All
252/3071 8.2%

(Best redshifts)
(69/1983 3.5%)

Hardness ratio

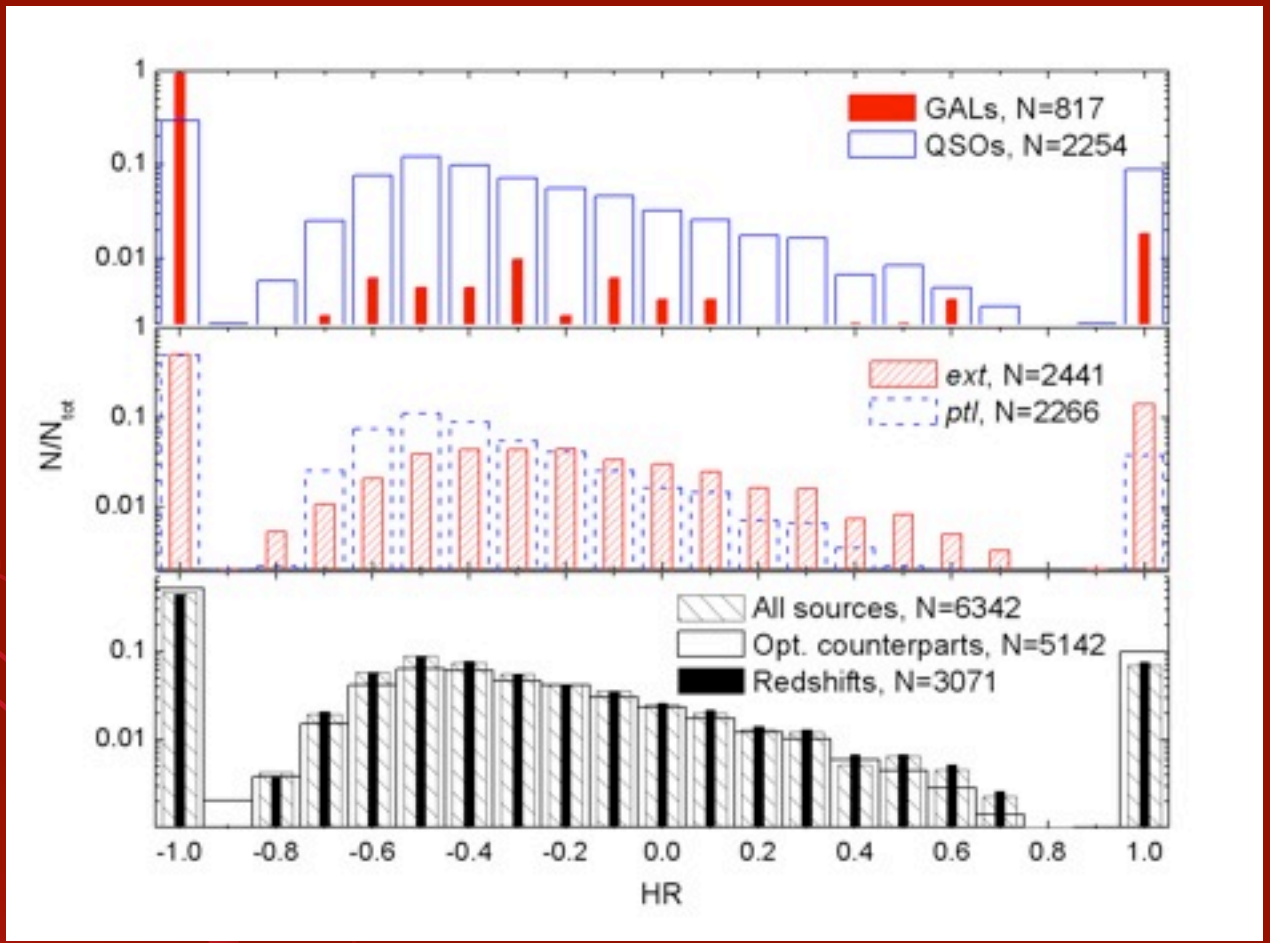

IRAC color-color plot

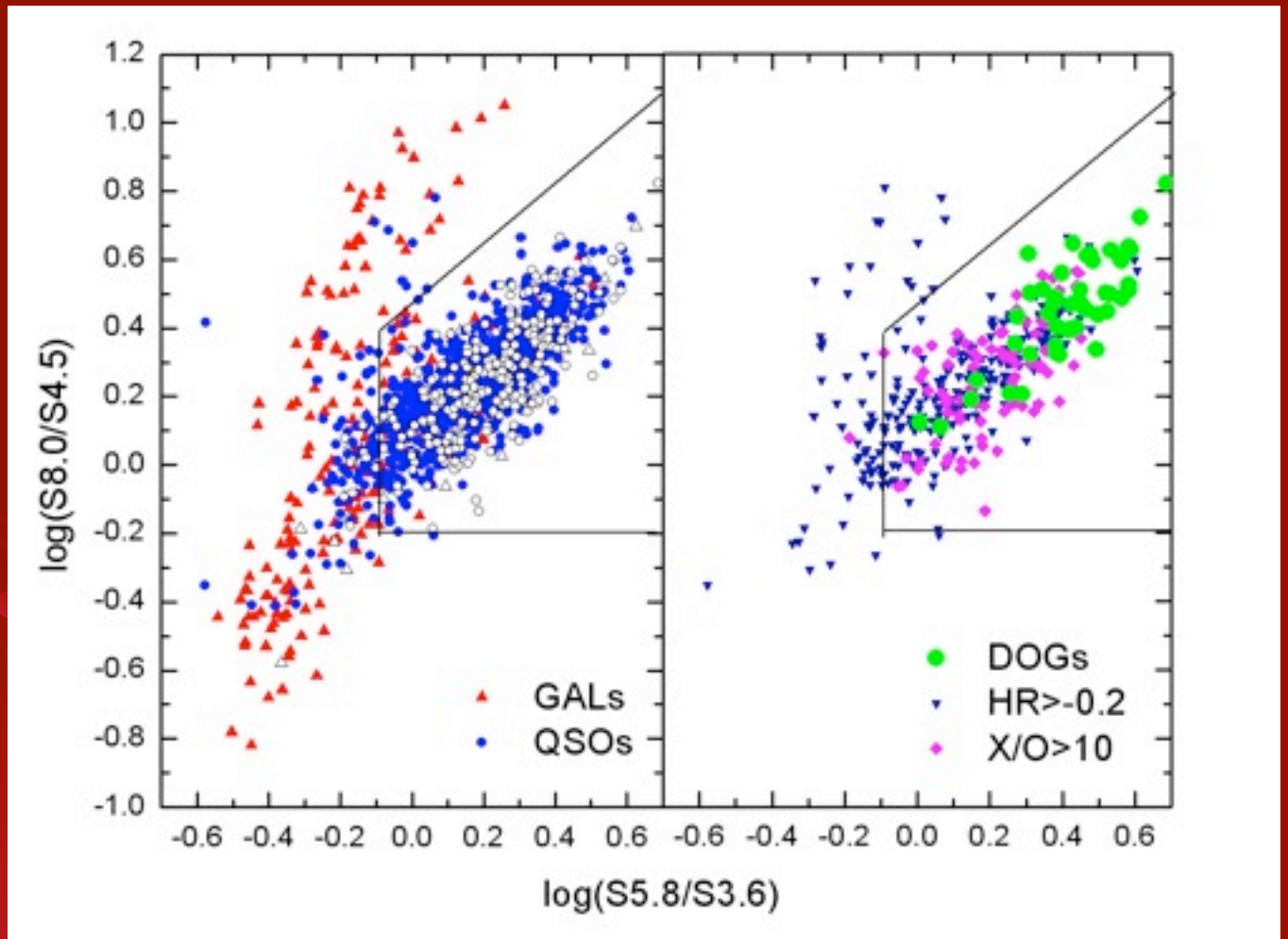

4 IRAC bands
51.6%

54 (21)
1.8% (1.1%)

Dust Obscured Galaxies (DOGs)
Dey et al. (2008)
<z>=1.99±0.45

Our DOGs
<z>= 1.67±0.39
(<z>= 1.54±0.34)

ALL
<z>= 1.27±0.75
(<z>= 1.18±0.80)

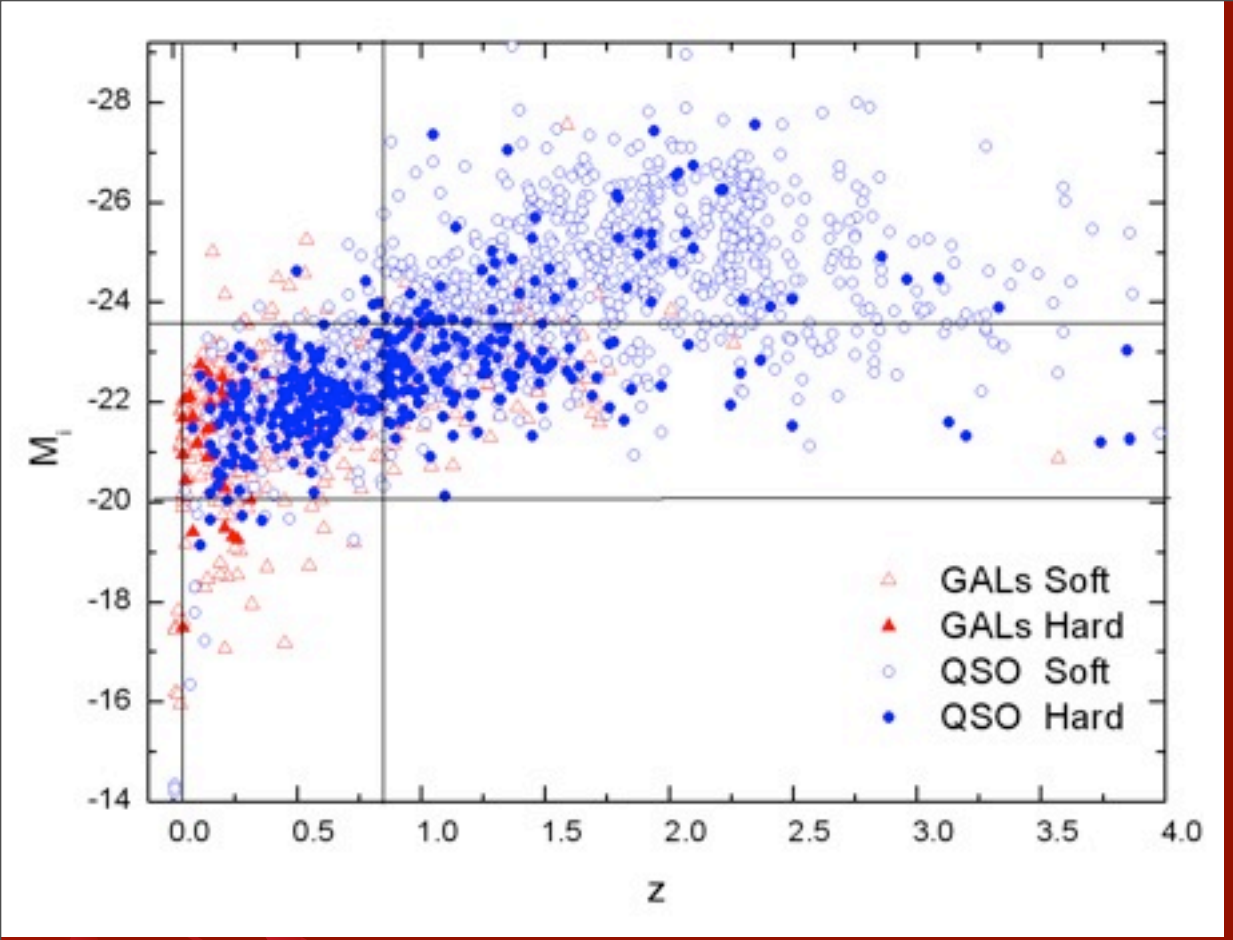

$$m^* = 5\log_{10} d_L + 25 + M_i^* + Q_{0.1}(z) + K_{0.1}(z)$$

m*<22.5

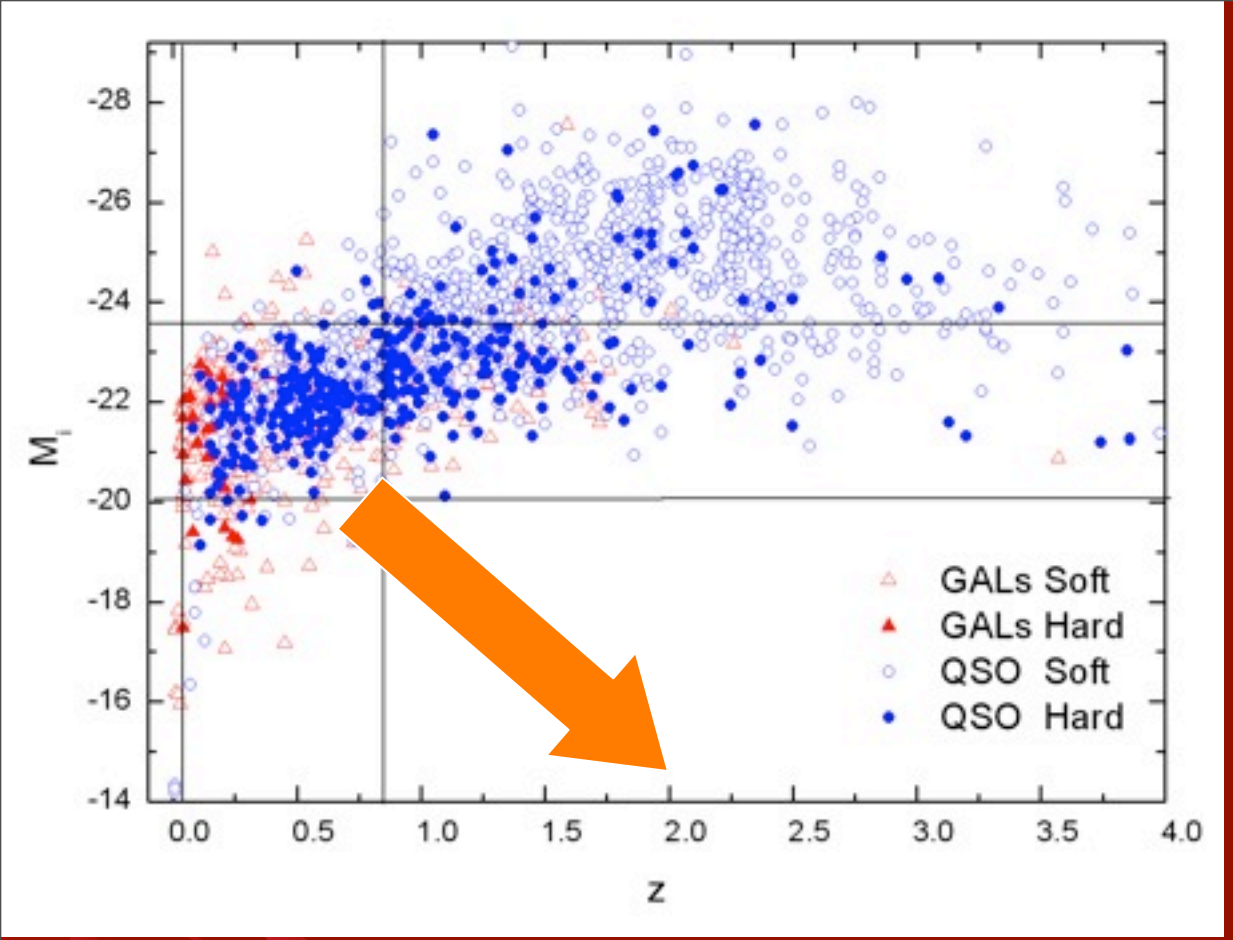

$$m^* = 5\log_{10} d_L + 25 + M_i^* + Q_{0.1}(z) + K_{0.1}(z)$$

m*<22.5

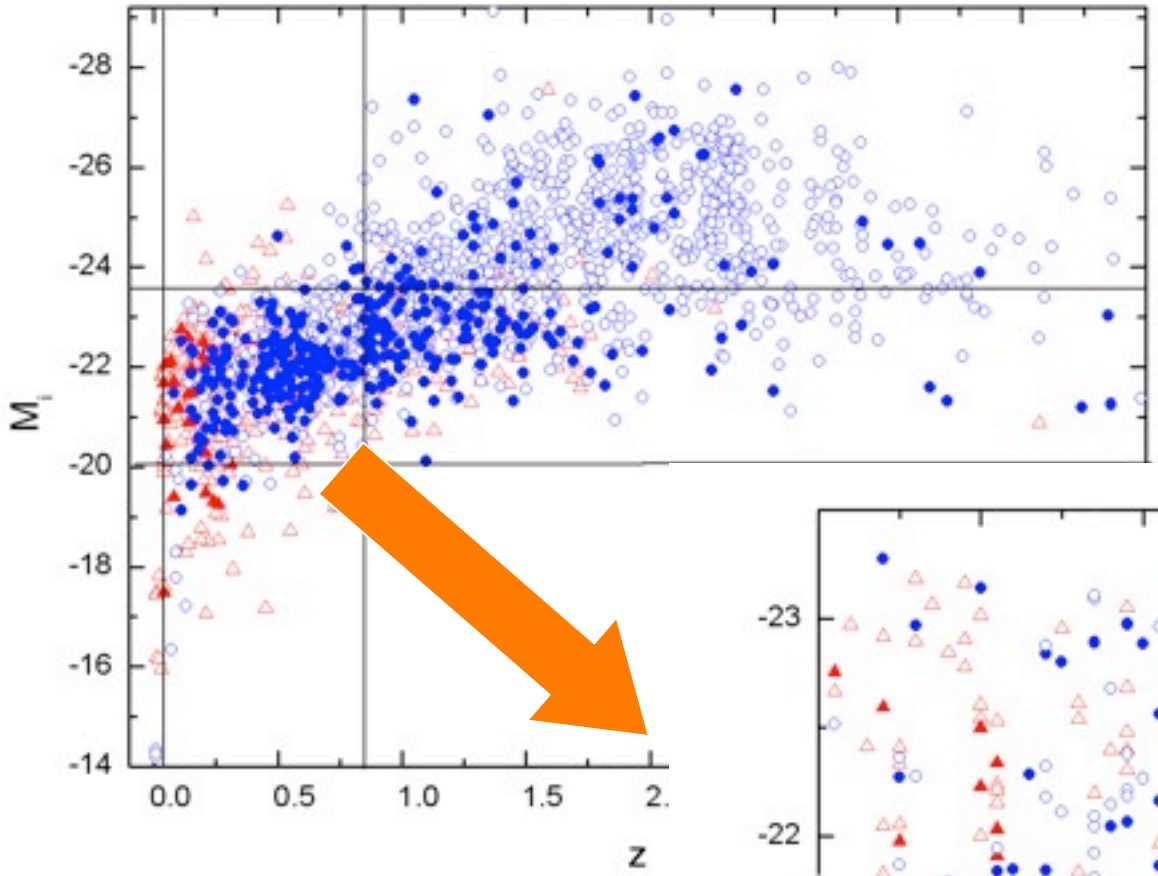

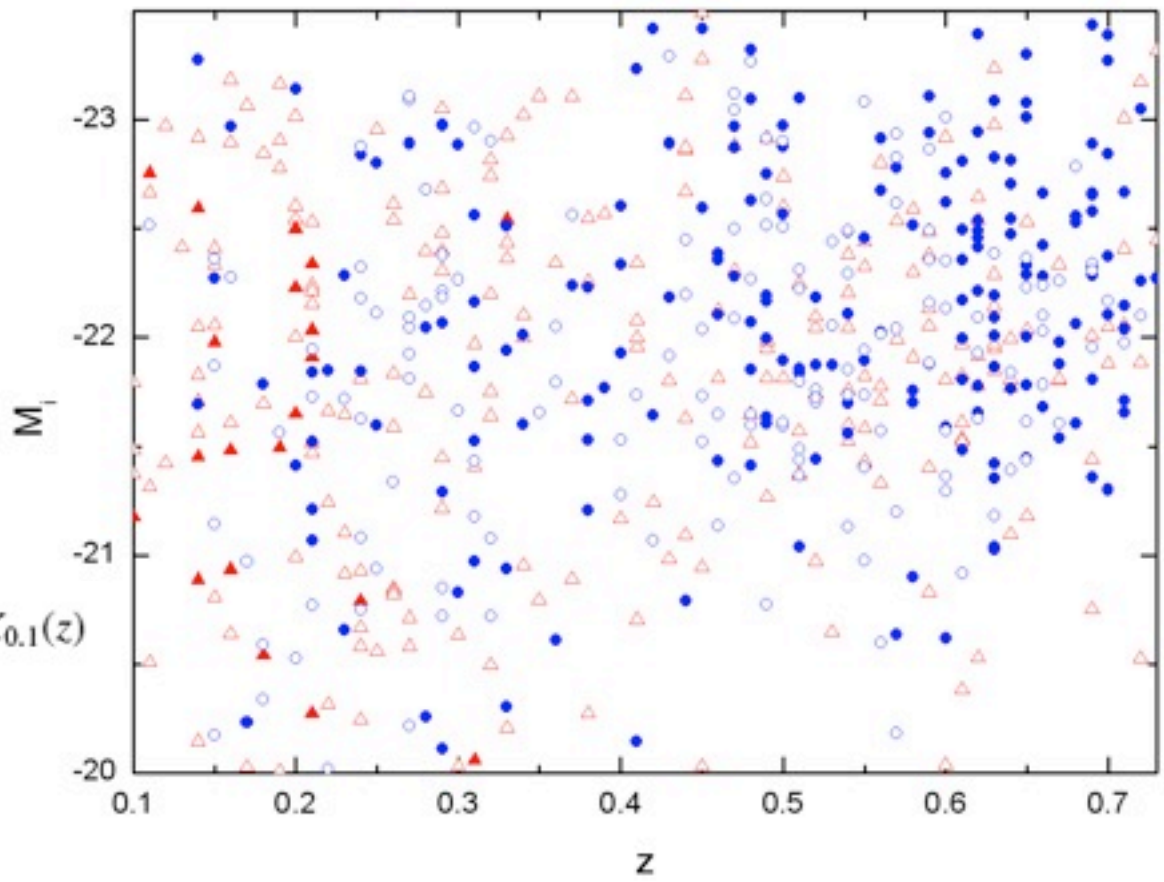

$$m^* = 5\log_{10} d_L + 25 + M_i^* + Q_{0.1}(z) + K_{0.1}(z)$$

m*<22.5

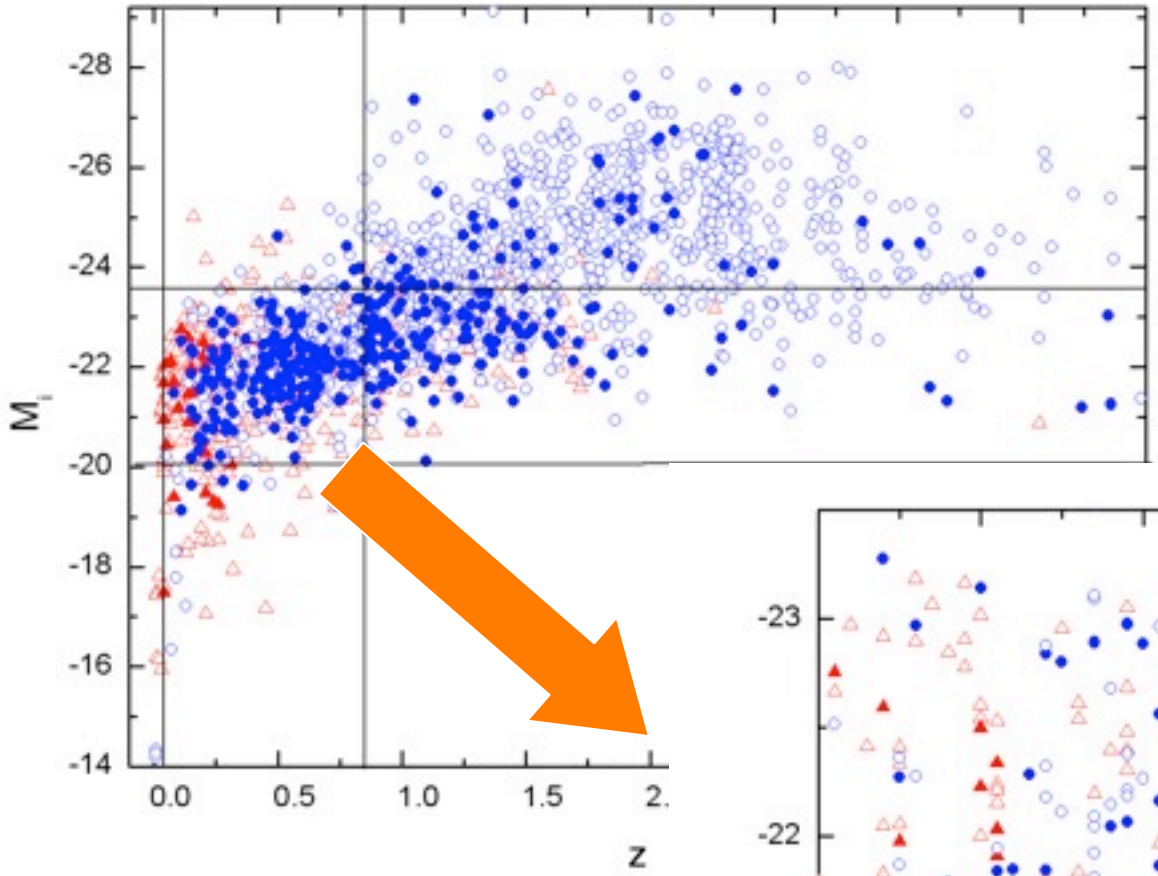

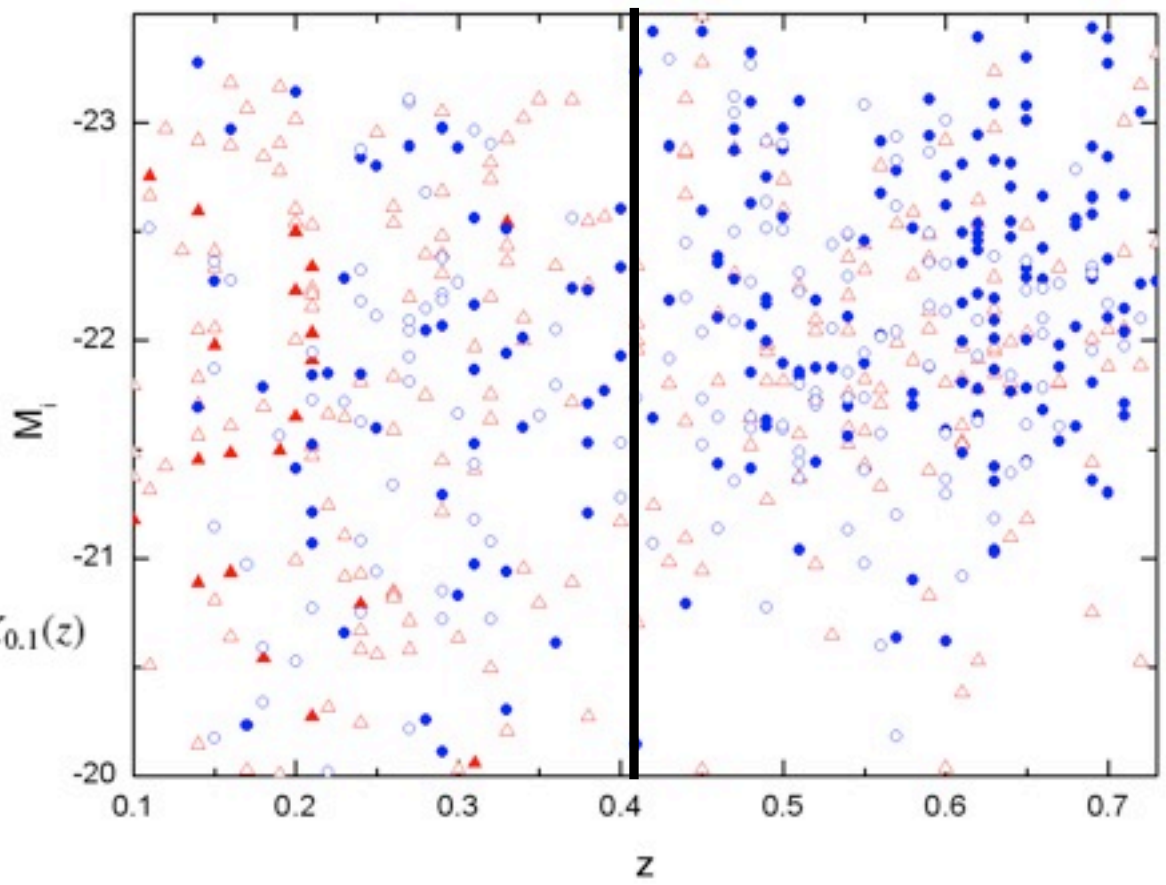

$$m^* = 5\log_{10} d_L + 25 + M_i^* + Q_{0.1}(z) + K_{0.1}(z)$$

m*<22.5

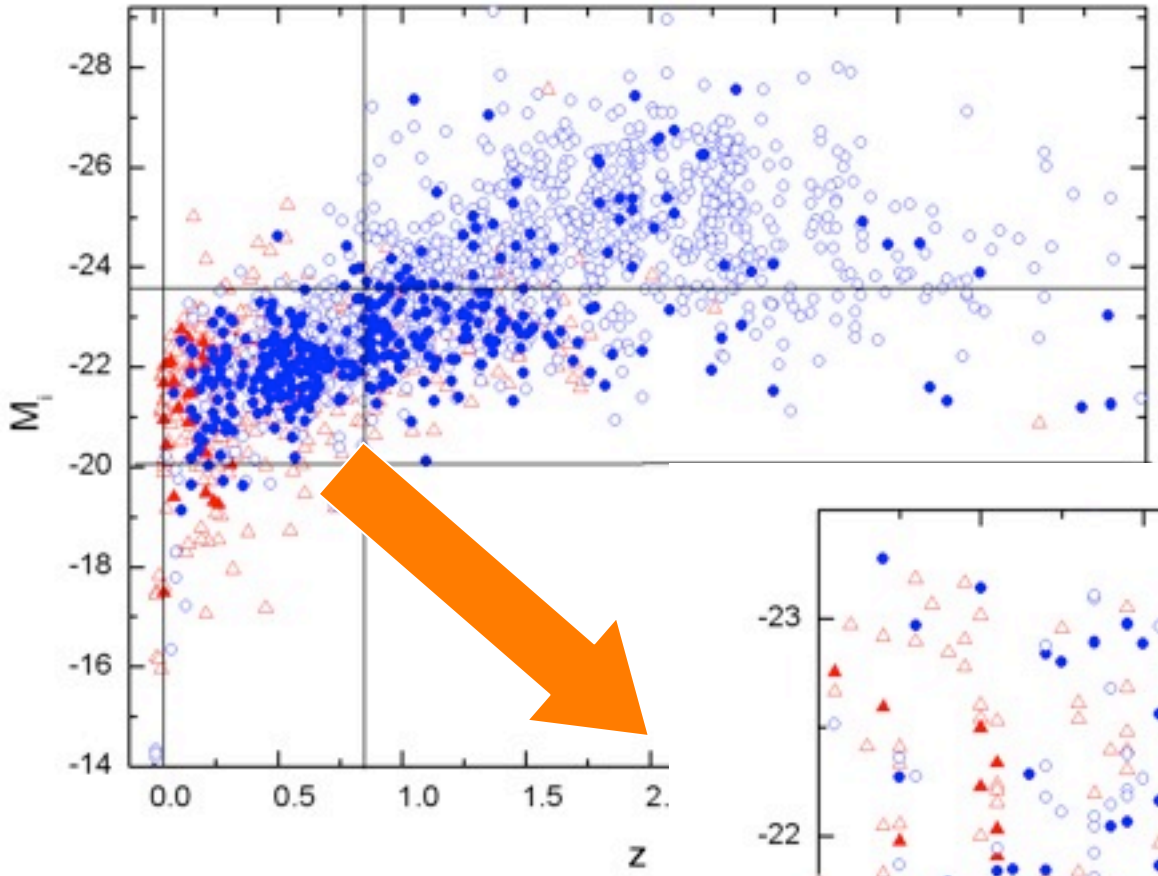

0.1<z<0.4; 0.4<z<0.7
GAL, QSO
Soft (HR<-0.2)
Hard (HR≥-0.2)
QSO_Soft (unobscured)
QSO_Hard (obscured)

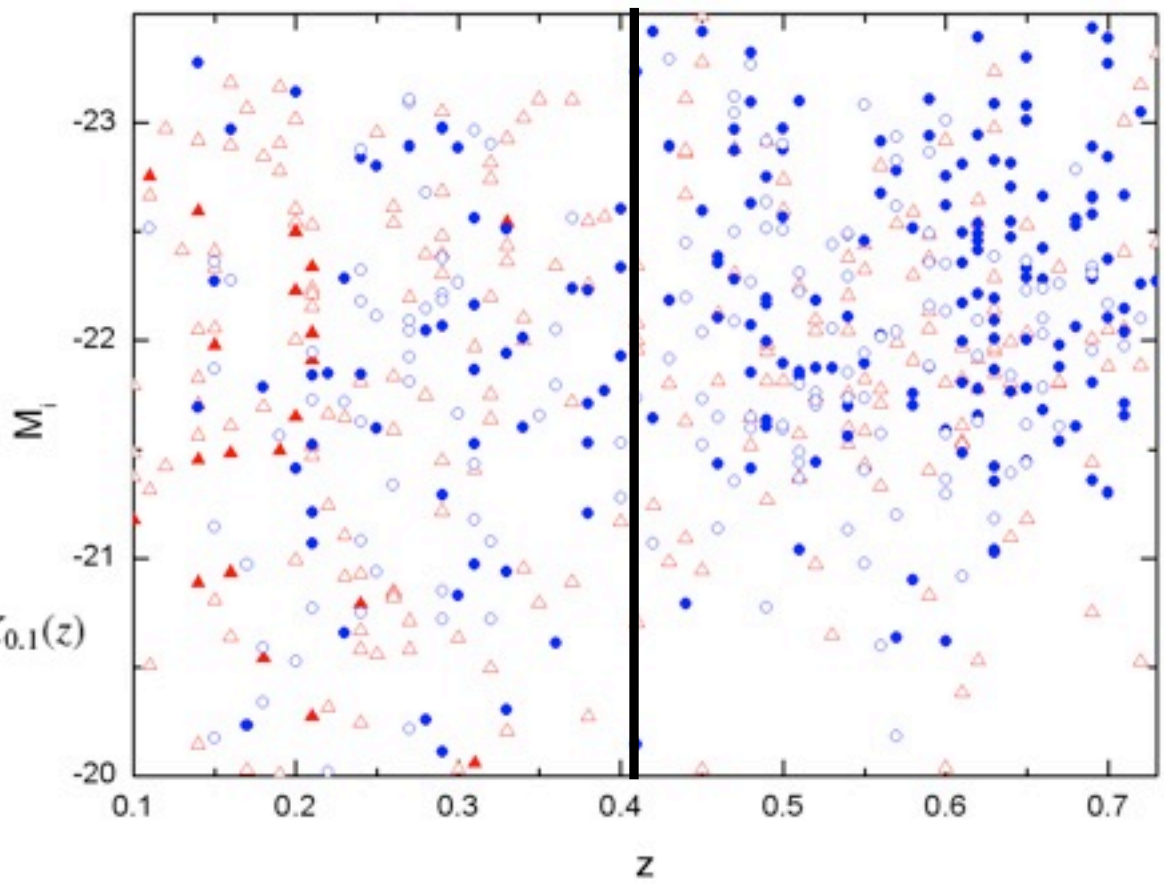

$$m^* = 5\log_{10} d_L + 25 + M_i^* + Q_{0.1}(z) + K_{0.1}(z)$$

m*<22.5

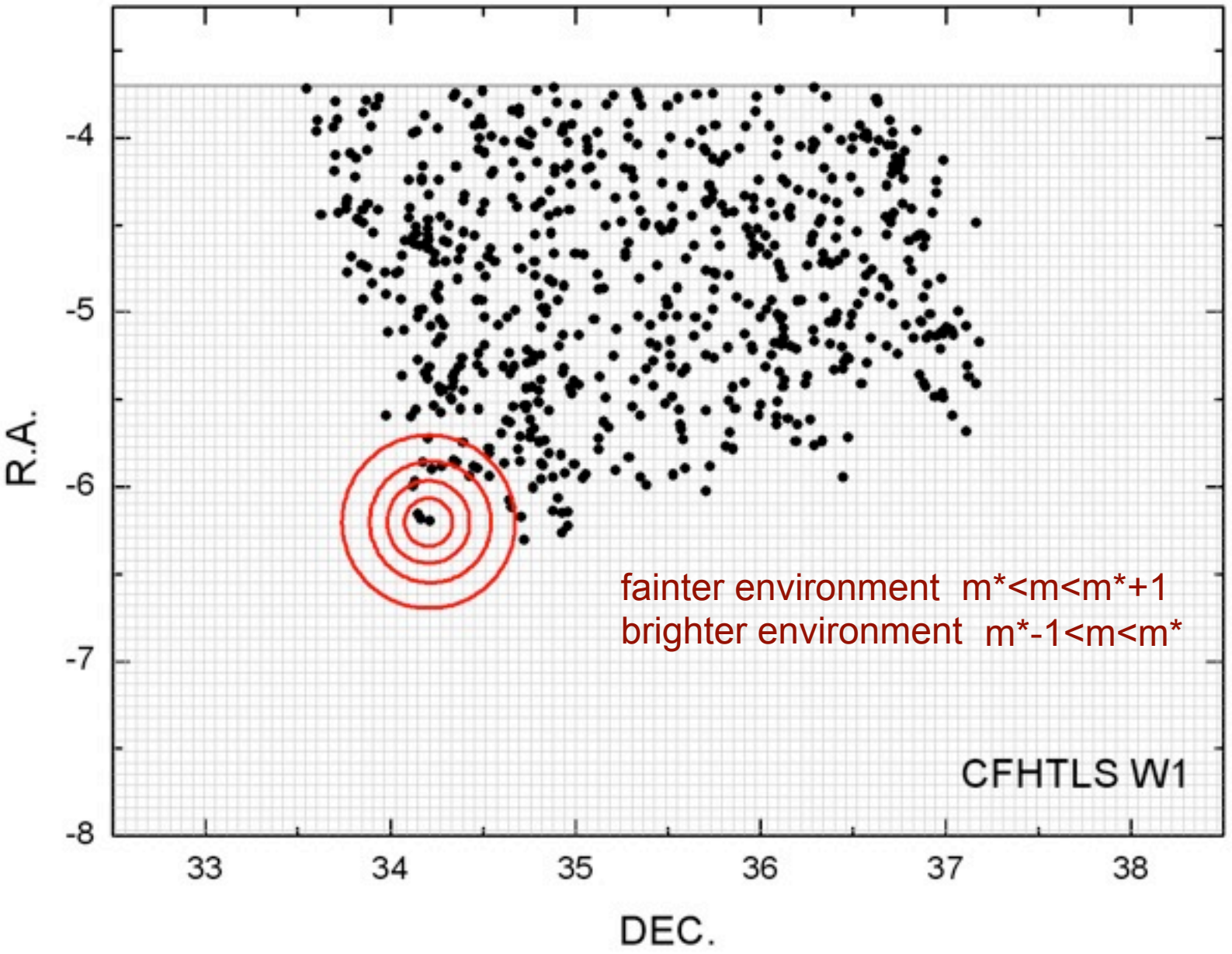
R.A.
-4
-5
-6
-7
-8
33
34
35
36
37
38
DEC.
fainter environment m*<m<m*+1
brighter environment m*-1<m<m*
CFHTLS W1

Overdensity measures

$$\delta_i = \frac{N_i}{f_i N_b} - 1$$

$$f_i = \frac{A_i}{A_b}$$

N_i is the total number of objects within i^{th} radial annulus of surface area A_i;

N_b is the local background counts, estimated in the spherical annulus between 4 and 5 Mpc, of surface area A_b;

f_i is the normalization factor that normalizes the background counts to the area of each spherical annulus

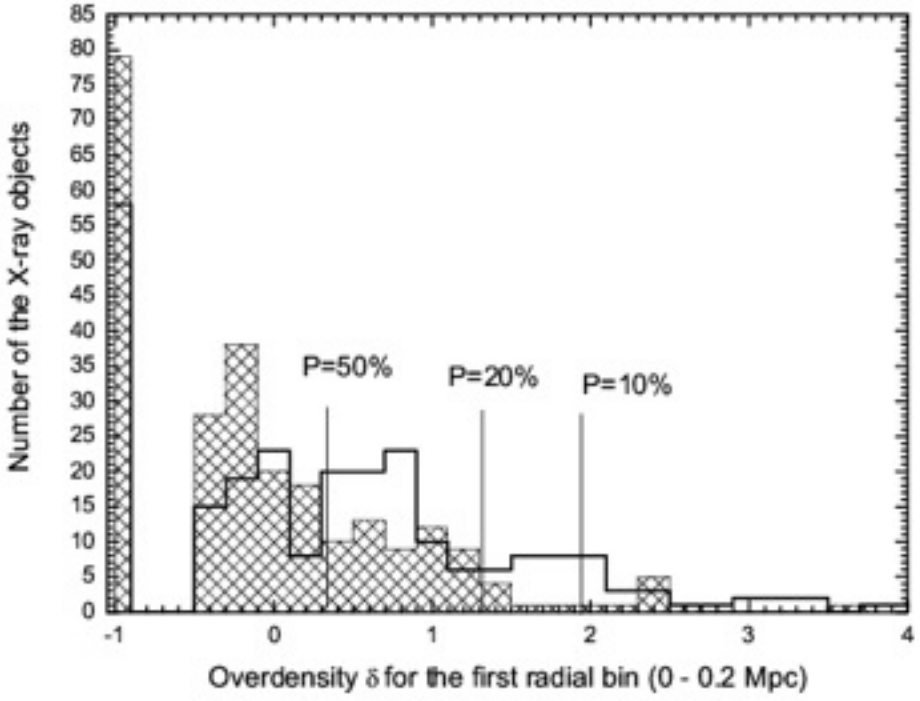

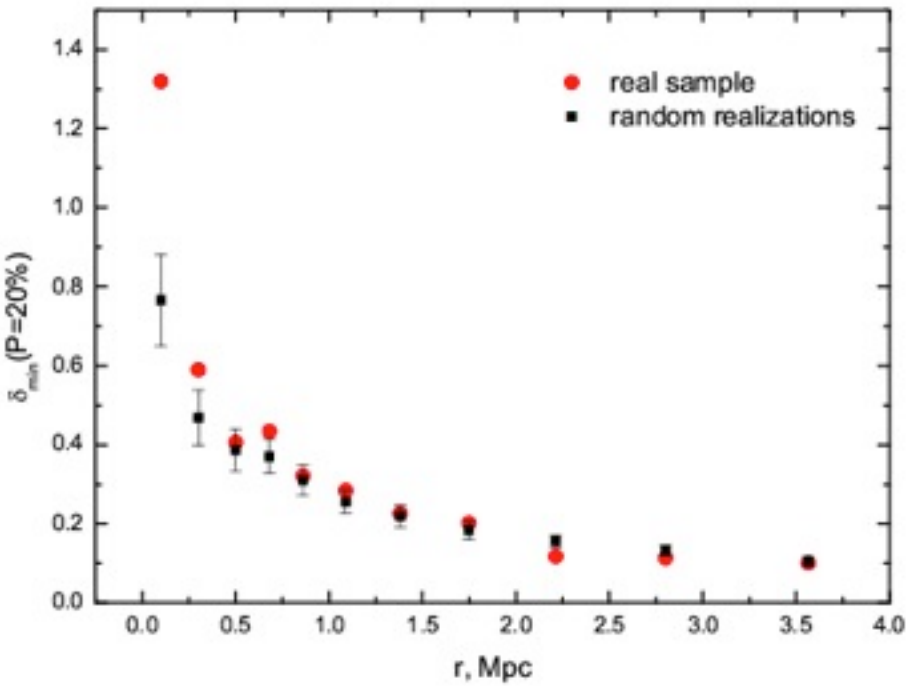

$$S/N = (\delta_{\min} - \langle \delta_{\min}^{\mathrm{rnd}} \rangle)/\sigma$$

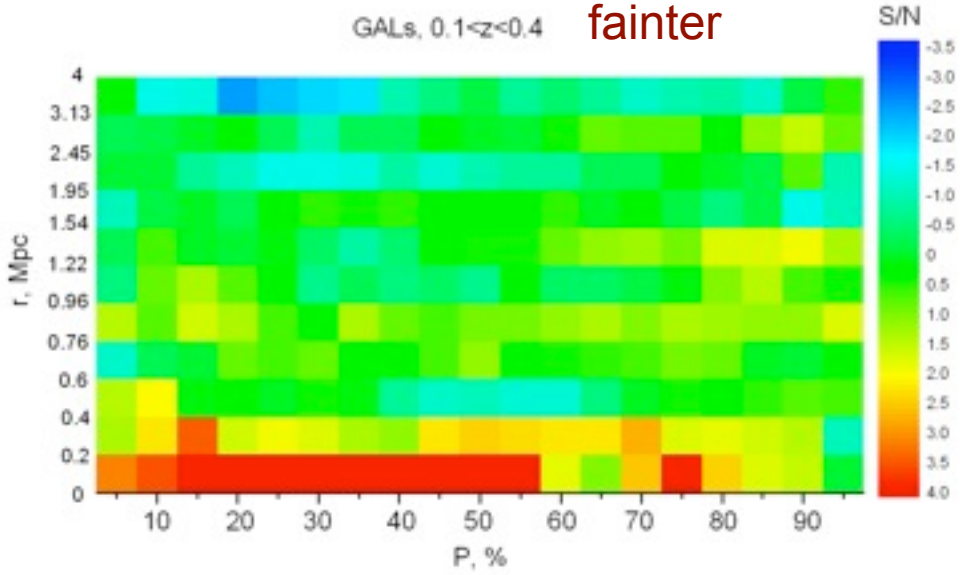

N=128

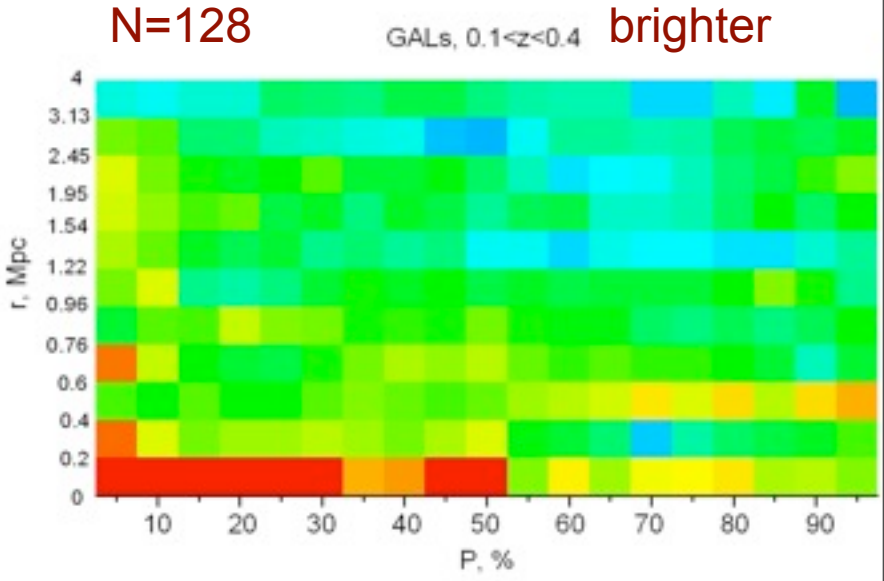

P=20%

	S/N	δ_{min}	S/N	δ_{min}
GAL	4.4	1.53	7.2	2.81
QSO	0.9	0.93	6.0	2.63

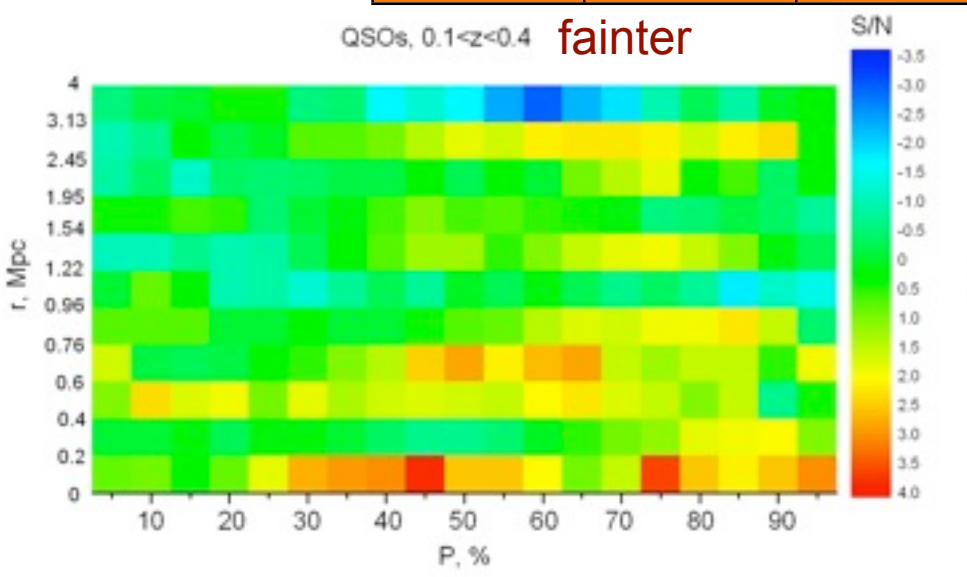

N=107

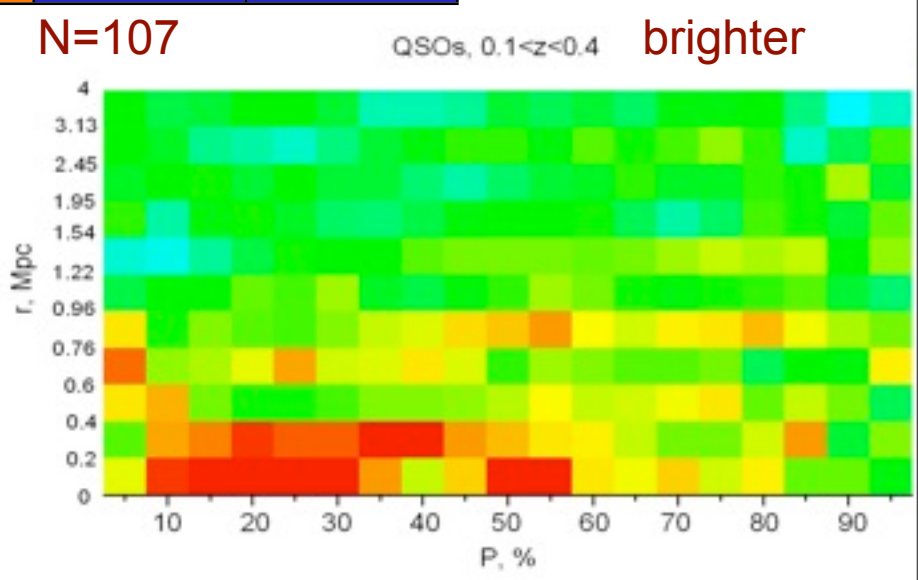

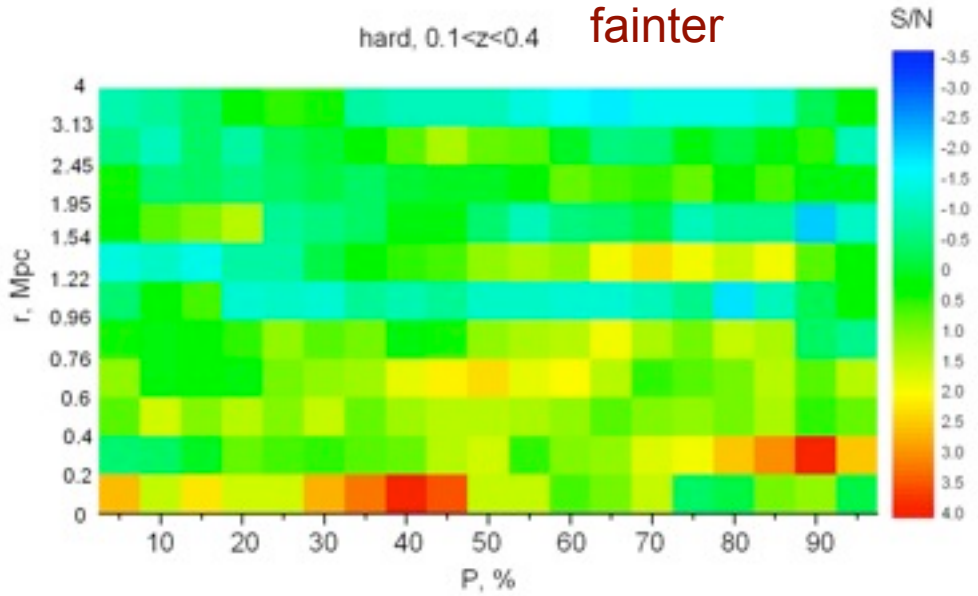

N=72

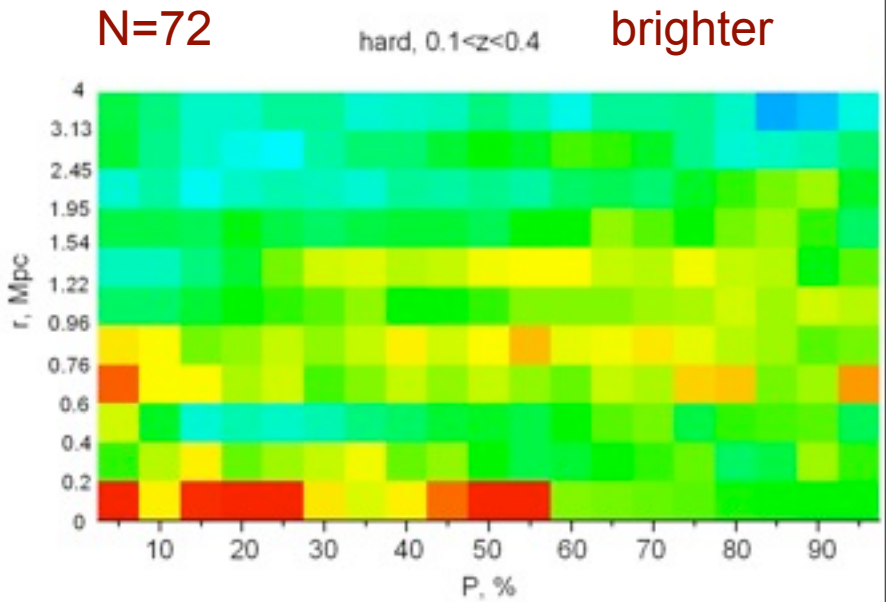

P=20%

	S/N	δ_{min}	S/N	δ_{min}
Hard	1.6	1.20	4.8	2.81
Soft	3.3	1.22	6.5	2.63

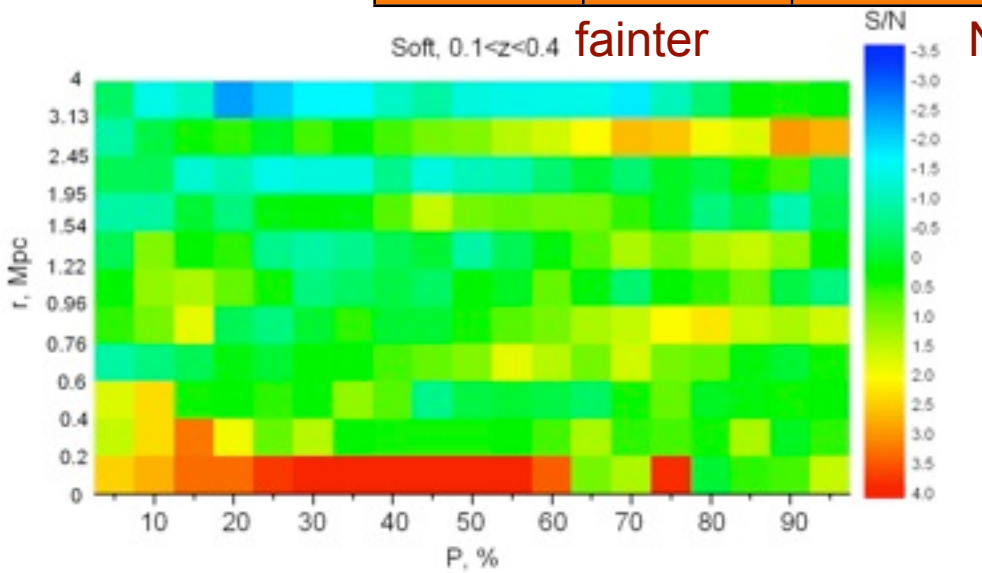

N=163

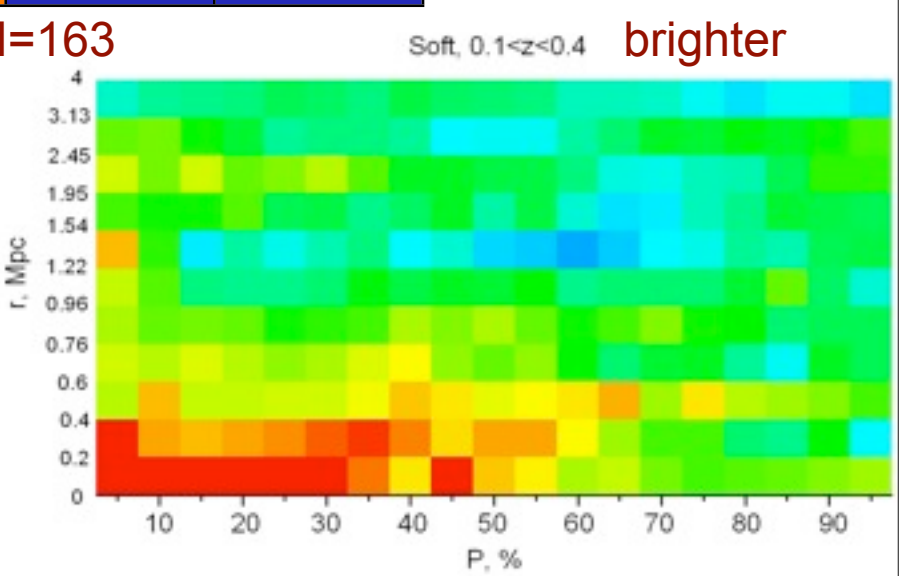

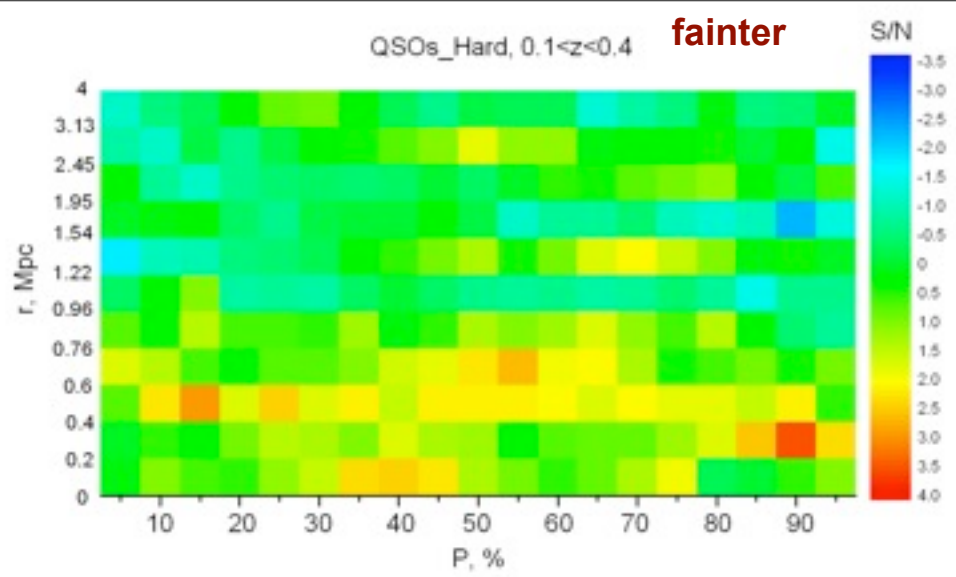

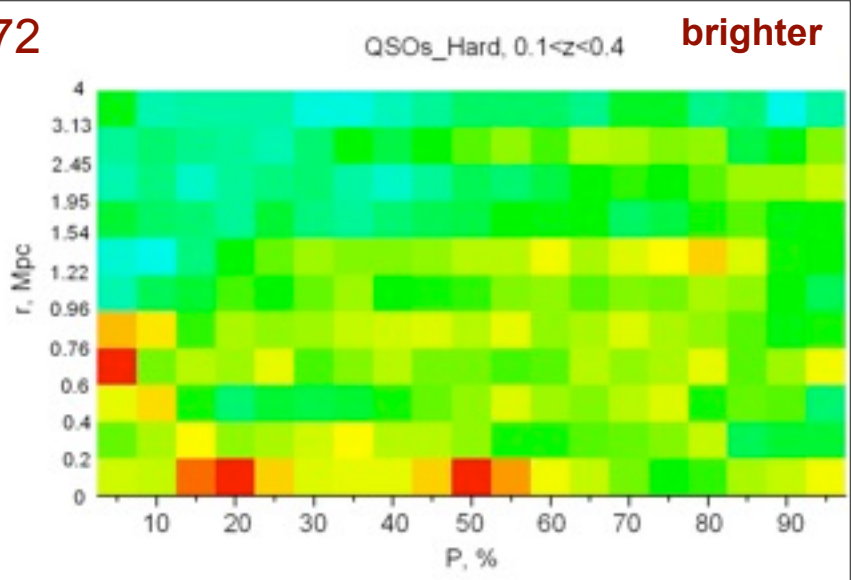

P=20%

	S/N	δ_{min}	S/N	δ_{min}
QSO_Hard	0.5	0.93	4.5	2.46
QSO_Soft	0.8	0.85	4.4	2.66

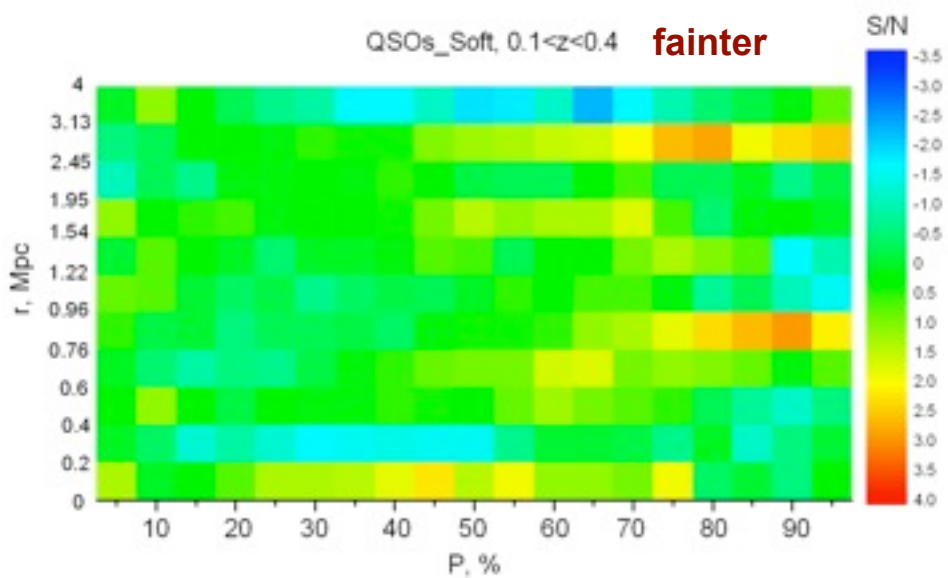

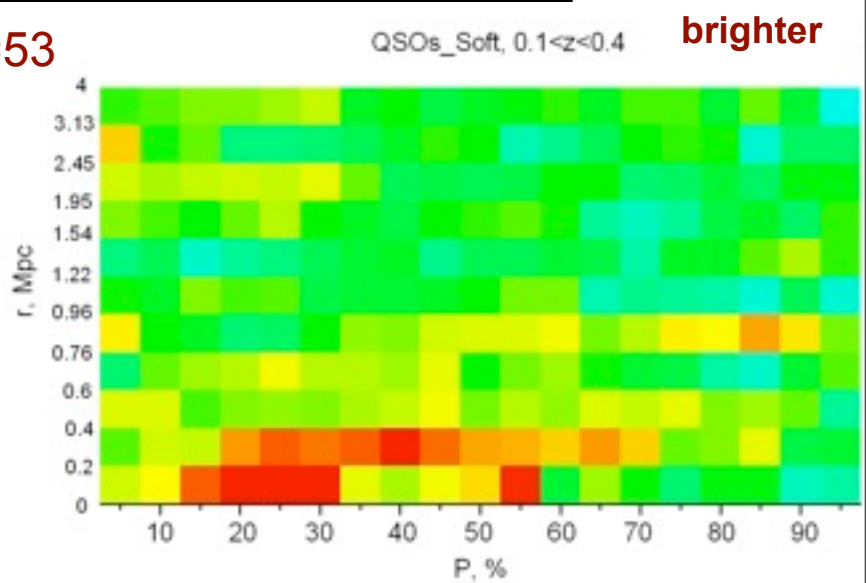

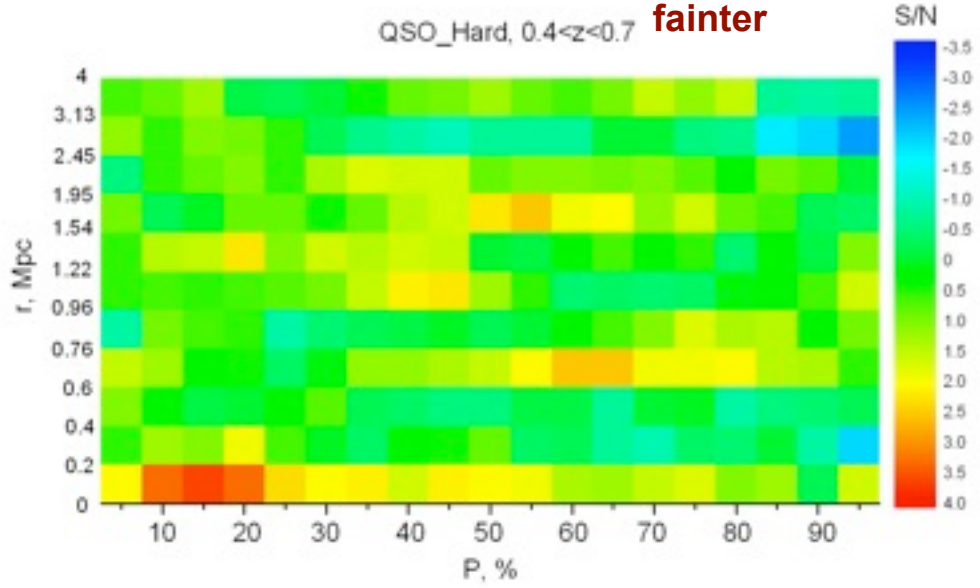

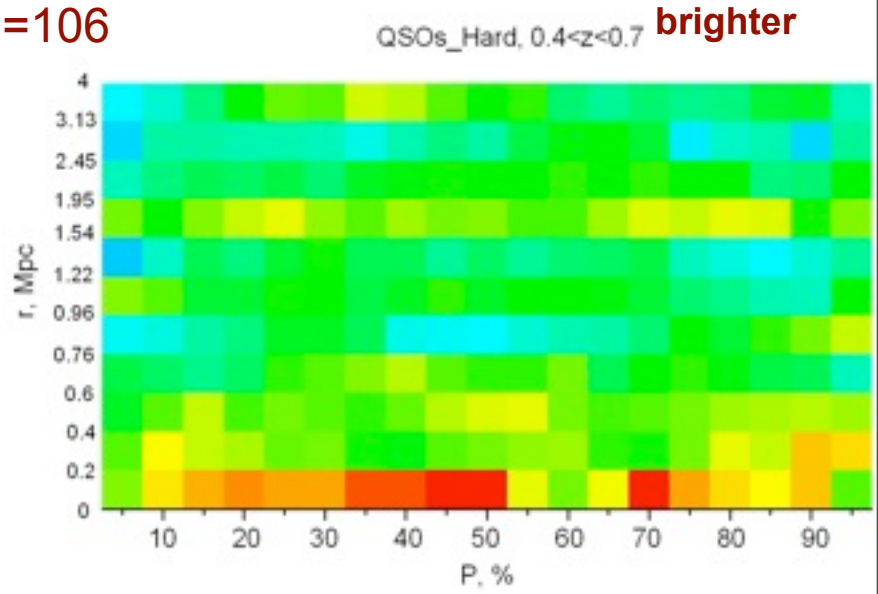

P=20%

	S/N	δ_{min}	S/N	δ_{min}
QSO_Hard	3.4	1.09	3.0	1.36
QSO_Soft	-0.6	0.5	-0.9	0.65

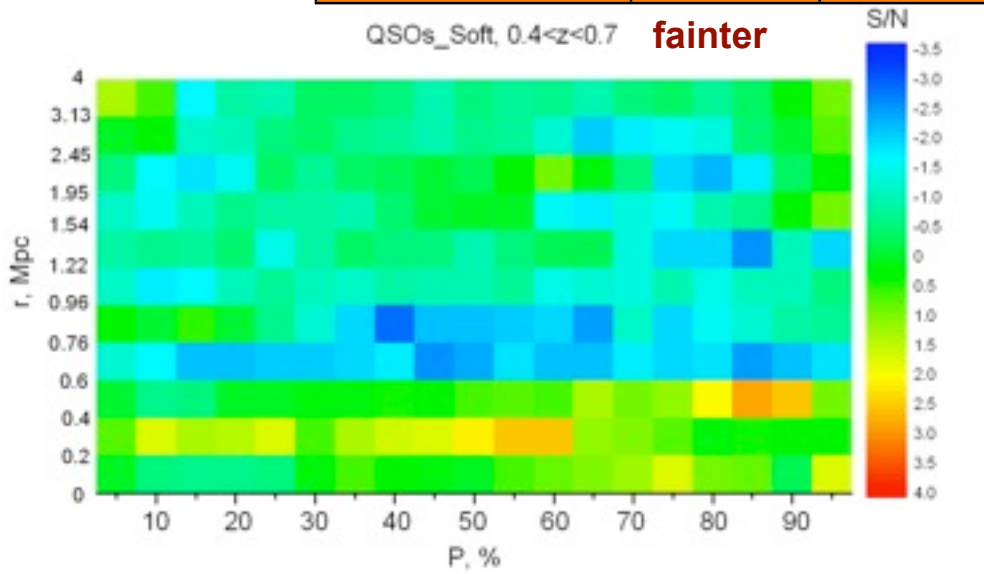

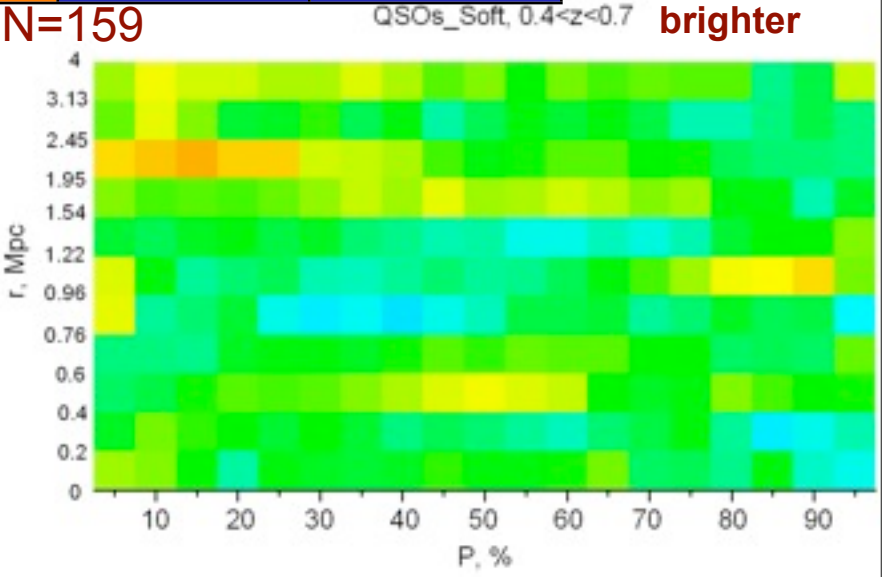

Conclusions

Conclusions

- We have estimated the photo-z using max. 11 bands with accuracies:

Conclusions

- We have estimated the photo-z using max. 11 bands with accuracies:
  - 4+ bands – σ=0.075; η=22%, N=4451;

Conclusions

- We have estimated the photo-z using max. 11 bands with accuracies:
  - 4+ bands – σ=0.075; η=22%, N=4451;
  - 7+ bands – σ=0.073; η=21.3%, N=3064;

Conclusions

- We have estimated the photo-z using max. 11 bands with accuracies:
  - 4+ bands – σ=0.075; η=22%, N=4451;
  - 7+ bands – σ=0.073; η=21.3%, N=3064;
    - ext - σ=0.057; η=10.6%;

Conclusions

- We have estimated the photo-z using max. 11 bands with accuracies:
  - 4+ bands – σ=0.075; η=22%, N=4451;
  - 7+ bands – σ=0.073; η=21.3%, N=3064;
    - ext - σ=0.057; η=10.6%;
    - ptl - σ=0.087; η=26.7%.

Conclusions

- We have estimated the photo-z using max. 11 bands with accuracies:
  - 4+ bands – σ=0.075; η=22%, N=4451;
  - 7+ bands – σ=0.073; η=21.3%, N=3064;
    - ext - σ=0.057; η=10.6%;
    - ptl - σ=0.087; η=26.7%.

Improving:

Conclusions

- We have estimated the photo-z using max. 11 bands with accuracies:
  - 4+ bands – σ=0.075; η=22%, N=4451;
  - 7+ bands – σ=0.073; η=21.3%, N=3064;
    - ext - σ=0.057; η=10.6%;
    - ptl - σ=0.087; η=26.7%.

Improving:

- sp-z control;

Conclusions

- We have estimated the photo-z using max. 11 bands with accuracies:
  - 4+ bands – σ=0.075; η=22%, N=4451;
  - 7+ bands – σ=0.073; η=21.3%, N=3064;
    - ext - σ=0.057; η=10.6%;
    - ptl - σ=0.087; η=26.7%.

Improving:

- sp-z control;
- the same aperture photometry for all bands;

Conclusions

- We have estimated the photo-z using max. 11 bands with accuracies:
  - 4+ bands – σ=0.075; η=22%, N=4451;
  - 7+ bands – σ=0.073; η=21.3%, N=3064;
    - ext - σ=0.057; η=10.6%;
    - ptl - σ=0.087; η=26.7%.

Improving:

- sp-z control;
- the same aperture photometry for all bands;
- We need more bands with uniform coverage!

Conclusions

- The X-ray point-like sources typically reside in overdense regions (>50%). X-ray sources can be found in a variety of environments.
- Overdensities defined by bright neighbours are significantly larger than those defined by faint neighbours.
- X-ray galaxies and QSOs appear to inhabit different environments: galaxies inhabit significant fainter and brighter overdensities but with a spatial scale up to 200 kpc , while QSOs only inhabit significant brighter overdensities with a much larger spatial extent.
- Unobscured and obscured QSOs are located in similar environments in $0.1<z<0.4$ range but in $0.4<z<0.7$ redshift range obscured QSOs prefer denser environment.